Neuron
Article

LTP Requires a Unique Postsynaptic SNARE Fusion Machinery

Sandra Jurado,[1,5] Debanjan Goswami,[1,5] Yingsha Zhang,[2] Alfredo J. Miñano Molina,[1,4] Thomas C. Südhof,[2,3] and Robert C. Malenka[1,*]
[1]Nancy Pritzker Laboratory, Department of Psychiatry and Behavioral Sciences
[2]Department of Molecular and Cellular Physiology
[3]Howard Hughes Medical Institute
Stanford University School of Medicine, 265 Campus Drive, Stanford, CA 94305, USA
[4]Centro de Investigación Biomédica en Red sobre Enfermedades Neurodegenerativas (CIBERNED) and Institut de Neurociencies and Departament de Bioquímica i Biología Molecular, Universitat Autònoma de Barcelona, 08193 Barcelona, Spain
[5]These authors contributed equally to this work
*Correspondence: malenka@stanford.edu
http://dx.doi.org/10.1016/j.neuron.2012.11.029

SUMMARY

Membrane fusion during exocytosis is mediated by assemblies of SNARE (soluble NSF-attachment protein receptor) and SM (Sec1/Munc18-like) proteins. The SNARE/SM proteins involved in vesicle fusion during neurotransmitter release are well understood, whereas little is known about the protein machinery that mediates activity-dependent AMPA receptor (AMPAR) exocytosis during long-term potentiation (LTP). Using direct measurements of LTP in acute hippocampal slices and an in vitro LTP model of stimulated AMPAR exocytosis, we demonstrate that the Q-SNARE proteins syntaxin-3 and SNAP-47 are required for regulated AMPAR exocytosis during LTP but not for constitutive basal AMPAR exocytosis. In contrast, the R-SNARE protein synaptobrevin-2/VAMP2 contributes to both regulated and constitutive AMPAR exocytosis. Both the central complexin-binding and the N-terminal Munc18-binding sites of syntaxin-3 are essential for its postsynaptic role in LTP. Thus, postsynaptic exocytosis of AMPARs during LTP is mediated by a unique fusion machinery that is distinct from that used during presynaptic neurotransmitter release.

INTRODUCTION

Experience-dependent modification of neural circuits is triggered by changes in neural activity patterns that initiate and ultimately produce long-term modifications of synapses. These functional adaptations, called synaptic plasticity, often rely on rapid changes in the composition of postsynaptic membranes, most notably changes in the number and in some cases the stoichiometry, of postsynaptic neurotransmitter receptors. At many excitatory synapses in the mammalian brain, synaptic plasticity requires the regulated trafficking of AMPA receptors (AMPARs), such that long-term depression (LTD) of synaptic transmission involves endocytosis of AMPARs and a consequent decrease in synaptic AMPAR number whereas NMDA receptor (NMDAR)-triggered long-term potentiation (LTP) involves exocytosis of AMPARs and a net increase in synaptic AMPARs (Bredt and Nicoll, 2003; Collingridge et al., 2004; Malinow and Malenka, 2002; Newpher and Ehlers, 2008; Shepherd and Huganir, 2007). Specific perisynaptic sites for endocytosis of synaptic AMPARs have been identified (Lu et al., 2007; Petrini et al., 2009) from where AMPARs may laterally diffuse into the postsynaptic density (PSD) at which they are stabilized by synaptic scaffolds (Henley et al., 2011; Kennedy and Ehlers, 2011; Opazo and Choquet, 2011). Although previous work suggests that SNARE proteins are required for the activity-dependent delivery of postsynaptic membranes and presumably AMPARs during LTP (Kennedy et al., 2010; Lledo et al., 1998; Lu et al., 2001), the specific SNARE proteins involved in regulated AMPAR exocytosis during LTP have not been identified. It is also not clear whether this same SNARE protein machinery mediates the constitutive AMPAR exocytosis that is required for maintaining basal synaptic strength. The distinction between the molecular mechanisms underlying constitutive versus regulated AMPAR exocytosis is particularly important given the critical involvement of LTP in many forms of experience-dependent plasticity (Malenka and Bear, 2004; Neves et al., 2008) and its use as a probe in defining pathological brain function in neuropsychiatric disorders (Clapp et al., 2012; Ehlers, 2012).

Much of our mechanistic understanding of SNARE-mediated fusion is derived from the study of neurotransmitter release at presynaptic nerve terminals. The vesicular R-SNARE protein synaptobrevin/VAMP interacts with two target Q-SNARE proteins, SNAP-25 and syntaxin-1, to form a transient complex that fuels membrane fusion by bringing the vesicle and plasma membranes into close apposition (Jahn et al., 2003; Jahn and Scheller, 2006; Rizo and Rosenmund, 2008; Südhof, 2004; Südhof and Rothman, 2009). SNARE proteins provide the energy for fusion, which also requires the SM (for Sec1/Munc18-like) protein Munc18-1 (Verhage et al., 2000). The actual exocytic fusion event is triggered when an action potential evoked increase in calcium activates a synaptotagmin, most commonly

synaptotagmin-1 (Fernández-Chacón et al., 2001; Südhof and Rothman, 2009). SNARE complex assembly is mediated by the SNARE motif, a conserved sequence that is present in one (syntaxin and synaptobrevin) or two copies (SNAP-25) in all SNARE proteins and forms tight four-helical bundles resistant to SDS denaturation (Hayashi et al., 1994; Sutton et al., 1998). SNARE-dependent interactions are promiscuous in vitro (Fasshauer et al., 1999; Yang et al., 1999) but exhibit a high degree of specificity in vivo (Südhof and Rothman, 2009).

An important cofactor for synaptotagmin-triggered presynaptic vesicle fusion is complexin (McMahon et al., 1995), a protein that both activates and clamps the SNARE complex in preparation for Ca^{2+}-triggered fusion during exocytosis (Giraudo et al., 2006; Huntwork and Littleton, 2007; Maximov et al., 2009; Reim et al., 2001; Tang et al., 2006; Xue et al., 2008, 2009; Yang et al., 2010). Recently, using a molecular replacement strategy in which complexin was manipulated in vivo as well as in cultured neurons, we demonstrated that postsynaptic complexin is required for the regulated delivery of AMPARs to synapses during LTP (Ahmad et al., 2012). This was a surprising result because previous work in cell culture had suggested that the NMDAR-triggered delivery of transferrin receptors to perisynaptic membranes required syntaxin-4 and that AMPARs are delivered to synapses by the same pathway during LTP (Park et al., 2004; Kennedy et al., 2010), yet syntaxin-4 does not bind to complexin (Pabst et al., 2000). Thus, the specific postsynaptic syntaxin required for AMPAR exocytosis during LTP has not been unequivocally identified. Similarly, the specific SNAP-25 homolog participating in the regulated exocytosis of AMPARs via SNARE-mediated fusion is also unknown. Both SNAP-23 and SNAP-25 have been suggested to play specific roles in the trafficking of NMDARs to synapses (Lau et al., 2010; Suh et al., 2010), while a neuronal role for the recently identified SNAP-47 (Holt et al., 2006) has not been explored.

Here, using shRNA-mediated knockdown (KD) of target proteins combined with a molecular replacement strategy (Schlüter et al., 2006; Xu et al., 2008) that allows molecular manipulations with high spatial and temporal resolution, we have performed a comprehensive analysis to decipher the specific molecular constituents of postsynaptic SNARE complexes that drive AMPAR exocytosis during LTP. This required generating effective and specific shRNAs to syntaxin-1, -3, and -4 and to SNAP-23, -25, and -47, and introducing these shRNAs into neurons in culture and in vivo. For all KD and rescue manipulations, we measured LTP in acute hippocampal slices, the preparation that has served as the gold standard for elucidating the properties and mechanisms of LTP (Malenka and Nicoll, 1999). Specifically, we knocked down syntaxin and SNAP-25 isoforms in vivo in CA1 pyramidal cells and prepared acute slices from these animals so that LTP could be directly assayed electrophysiologically under experimental conditions in which only postsynaptically located versions of the targeted proteins were affected (Ahmad et al., 2012). In parallel, the identical molecular manipulations were performed in dissociated hippocampal cell cultures to directly quantify effects on NMDAR-triggered increases in endogenous AMPAR surface expression, a cell culture model of LTP (Kennedy et al., 2010; Lu et al., 2001; Park et al., 2004; Passafaro et al., 2001). By performing experiments in two different preparations using two different measurements and focusing on the trafficking of endogenous AMPARs, we minimized the possibility of generating spurious results.

Our results demonstrate that syntaxin-3, but not syntaxin-1 or -4, is required for regulated AMPAR delivery to synapses during LTP. Mutagenesis of syntaxin-3 and syntaxin-4 provided evidence that syntaxin-3's interaction with complexin is essential for its function in LTP, consistent with previous results (Ahmad et al., 2012). KDs of SNAP-25 and SNAP-47, but not of SNAP-23, impaired LTP. However, the SNAP-25 KD also decreased NMDARs at synapses to a degree that was sufficient to impair LTP induction. In contrast, KD of SNAP-47 altered neither basal AMPAR- nor NMDAR-mediated synaptic responses, but specifically impaired regulated AMPAR exocytosis during LTP. Partial truncation of the SNAP-47 C terminus revealed that a SNARE-dependent interaction is critical for its role in LTP. Finally, using synaptobrevin-2 knockout mice, we present evidence for a postsynaptic role for this vesicle SNARE in NMDAR-triggered AMPAR exocytosis. Together, these results identify critical roles for syntaxin-3, SNAP-47, and synaptobrevin-2 as components of a unique postsynaptic SNARE-mediated vesicle fusion machinery that is required for the regulated delivery of AMPARs to the plasma membrane during LTP.

RESULTS

Postsynaptic Syntaxin-3 Is Required for AMPAR Delivery during LTP

To identify the essential components of postsynaptic SNARE-complexes that mediate activity-dependent delivery of AMPARs to the plasma membrane during LTP, we generated effective short-hairpin RNAs (shRNAs) targeting SNARE proteins (see Figure S1 available online). These were cloned into a multipromoter lentivirus that allows efficient knockdown and simultaneous expression of shRNA-resistant versions of the targeted proteins (Figure 1A; Pang et al., 2010). These lentiviruses were used in two preparations that allowed complementary measures of AMPAR trafficking during LTP. In a neuronal culture model of LTP (Ahmad et al., 2012; Kennedy et al., 2010; Lu et al., 2001; Park et al., 2004; Passafaro et al., 2001), activation of NMDARs by bath application of the coagonist glycine causes an increase in the surface expression of endogenous GluA1-containing AMPARs compared to untreated control cells (Figure 1B: control 100.0% ± 2.9%, n = 26; glycine 217.0% ± 9.9%, n = 26). This change was associated with an increase in the amplitude and frequency of miniature EPSCs (Figure S2A), and was prevented by coapplication of either D-APV (25 μM), an NMDAR antagonist, or KN62 (1 μM), an inhibitor of calcium/calmodulin-dependent protein kinase 2 (CaMKII) (Figure S2B). Thus, this model of LTP mimics key features of NMDAR-dependent LTP in hippocampal CA1 pyramidal cells (Malenka and Nicoll, 1999). However, because dissociated neurons in culture are prepared from the brains of embryonic or newborn mice and do not faithfully form normal brain circuits (Soler-Llavina et al., 2011), excitatory synapses in these cultures are likely different from mature

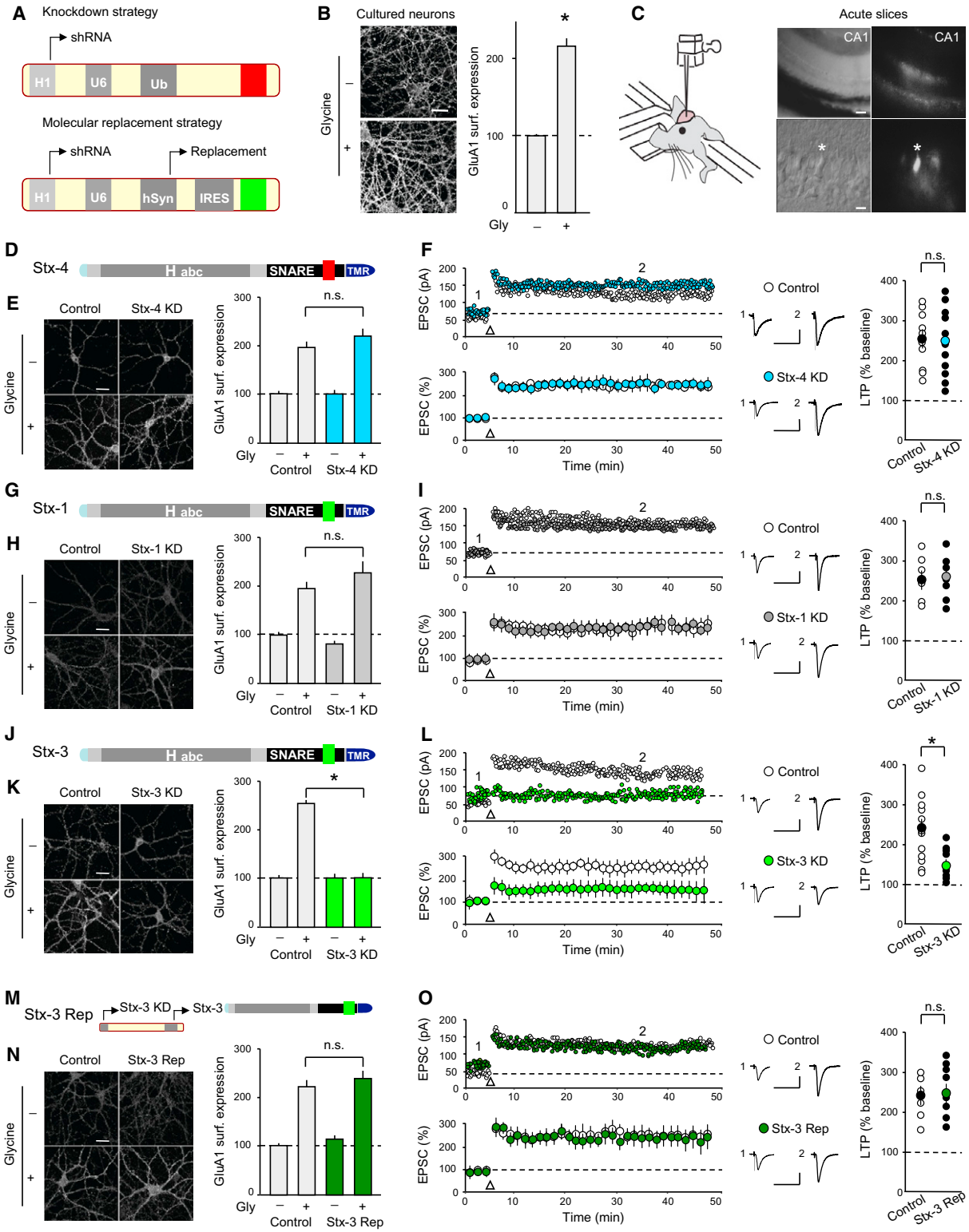

Figure 1. Postsynaptic Syntaxin-3 Is Required for Surface AMPAR Delivery during LTP

(A) Schematics of lentivirus vectors.

(B) Images of cultured hippocampal neurons (left panels) and summary graph (right panel) showing surface GluA1 staining following glycine treatment.

(C) Schematic showing in vivo injection of lentiviruses. DIC (left panels) and fluorescence (right panels) images from acute hippocampal slice showing GFP-expressing CA1 pyramidal cells (upper/lower panel scale bar: 50 μm/10 μm).

(legend continued on next page)

synapses in situ. Therefore, it was important to determine whether results from the culture model of LTP could be replicated when mature synapses that had undergone the identical molecular manipulations in vivo were studied. To accomplish this task, we stereotactically injected the same lentiviruses into the hippocampal CA1 region of 3-week-old mice (Figure 1C) in a manner that only CA1 pyramidal cells were infected (Ahmad et al., 2012). Animals were sacrificed 10–14 days later and whole-cell voltage-clamp recordings were made from visually identified CA1 pyramidal cells in standard acute hippocampal slices. This approach allowed us to directly test the effects of purely postsynaptic manipulations of SNARE proteins on LTP in mature synapses.

We initially focused on syntaxins, which are plasma membrane SNAREs containing a conserved N-terminal sequence that mediates binding to proteins of the Sec1/Munc18 family (SM proteins), followed by an Habc domain, a SNARE motif, and a transmembrane region at its C terminus (Figure 1D). Because syntaxin-4 (Stx-4) was proposed to be the key syntaxin defining a site at which activity-dependent exocytosis occurs in dendritic spines during LTP (Kennedy et al., 2010), we first examined the consequences of a Stx-4 knockdown (Stx-4 KD). Surprisingly, the Stx-4 KD had no effect on glycine-induced increases in GluA1 surface expression in cell culture (Figure 1E: control, 102.0% ± 4.2%, n = 35; control/glycine, 190.0% ± 12.5%, n = 35; Stx-4 KD, 100.0% ± 4.9%, n = 35; Stx-4 KD/glycine, 212.0% ± 15.7%, n = 35), nor did it impair LTP measured in acute slices (Figure 1F: control, 247.0% ± 23.0%, n = 10; Stx-4 KD, 245.0% ± 21.0%, n = 11).

We next examined the consequences of knocking down syntaxin-1 (Stx-1) or -3 (Stx-3), which, in contrast to Stx-4, exhibit robust binding to complexin mediated by a 12 amino acid stretch in the middle of the SNARE motif (Figures 1G and 1J; Pabst et al., 2000). The Stx-1 KD had no effect on glycine-induced LTP in culture (Figure 1H: control, 100.0% ± 5.6%, n = 24; control/glycine, 190.0% ± 14.7%, n = 24; Stx-1 KD, 82.0% ± 5.3%, n = 31; Stx-1 KD/glycine, 223.0% ± 21.9%, n = 32) or on LTP examined in acute slices following in vivo Stx-1 KD (Figure 1I: control, 255.0% ± 22.0%, n = 6; Stx-1 KD, 264.0% ± 20.0%, n = 6). In contrast, the Stx-3 KD significantly impaired both glycine-induced increases in GluA1 surface expression in culture (Figure 1K: control, 102.0% ± 4.2%, n = 35; control/glycine, 253.0% ± 5.0%, n = 35; Stx-3 KD, 104.0% ± 6.3%, n = 35; Stx-3 KD/glycine 102.0% ± 5.7%, n = 35) and LTP recorded in acute slices (Figure 1L: control, 230.0% ± 23.0%, n = 12; Stx-3 KD, 140.0% ± 21.0%, n = 9). Importantly, the block of glycine-induced "LTP" in culture as well as the impairment in LTP following in vivo postsynaptic Stx-3 KD were fully rescued by simultaneous expression of shRNA-resistant full length Stx-3 (Stx-3 Rep; Figure 1M) (Figure 1N: control, 100.0% ± 5.0%, n = 32; control/glycine, 218.0% ± 11.4%, n = 34; Stx-3 Rep, 115.0% ± 4.1%, n = 36; Stx-3 Rep/glycine, 237.0% ± 12.3%, n = 33; Figure 1O; control 240.0% ± 23.0%, n = 6; Stx-3 Rep 245.0% ± 22.0%, n = 8). These results suggest that off-target effects of the Stx-3 shRNA are unlikely to account for its effects on LTP, and that Stx-3, but not Stx-1 or Stx-4, is critical for AMPAR delivery to the postsynaptic plasma membrane during LTP.

Postsynaptic Syntaxin-3 Is Not Required for Basal Synaptic Transmission or Constitutive Transferrin Receptor Recycling

To further define the role of postsynaptic Stx-3 in LTP, we assessed its subcellular localization in dendrites using structured illumination microscopy (Gustafsson et al., 2008). Costaining of permeabilized cultured neurons with antibodies against endogenous Stx-3 and PSD-95, a major constituent of excitatory synapses, revealed punctate Stx-3 staining throughout the soma and dendrites (Figure 2A; Movie S1). Stx-3 was often found adjacent to PSD-95 puncta, consistent with recent studies using immunogold labeling of syntaxins in hippocampal slices and cultured neurons (J.H. Tao-Cheng et al., 2012, Soc. Neurosci., abstract). The relatively ubiquitous distribution of Stx-3 in dendrites is similar to the ubiquitous distribution of presynaptic SNARE proteins, which are not specifically enriched in presynaptic boutons or active zones (Südhof, 2012).

(D) Schematic of Stx-4 showing its functional domains; (Habc, Habc domain; SNARE, soluble NSF-attachment protein receptor motif; TMR, transmembrane region; red indicates non-complexin-binding sequence).
(E) Sample images and summary graph (mean ± SEM) of glycine-induced changes in surface GluA1 in control and Stx-4 KD cultured neurons.
(F) Sample experiments (top) and summary graphs (bottom) of LTP in control and Stx-4 KD CA1 pyramidal cells, both recorded from slices prepared from animals injected with Stx-4 shRNA lentiviruses. In this and all subsequent figures: arrow indicates tetanic stimulation; sample averaged EPSCs during the baseline (1) and 35 min post-LTP induction (2) are shown next to the LTP graphs. Right panel shows scatter plots of individual experiments with mean ± SEM indicated by symbol with different color.
(G) Schematic of Stx-1 structure (complexin binding sequence is indicated in green).
(H) Sample images and summary graph of glycine-induced changes in surface GluA1 in control and Stx-1 KD cultured neurons.
(I) Sample experiments (top) and summary graphs (bottom) of LTP in control and Stx-1 KD CA1 pyramidal cells. Right panel shows scatter plots of individual experiments with mean ± SEM.
(J) Schematic of Stx-3 (complexin binding sequence in green).
(K) Sample images and summary graph of glycine-induced changes in surface GluA1 in control and Stx-3 KD cultured neurons.
(L) Sample experiments (top) and summary graphs (bottom) of LTP in control and Stx-3 KD CA1 pyramidal cells. Right panel shows scatter plots of individual experiments with mean ± SEM.
(M) Schematic illustrating the replacement strategy.
(N) Sample images and summary graph showing rescue of glycine-induced increases in surface GluA1 by Stx-3 in Stx-3 KD cultured neurons.
(O) Sample experiments (top) and summary graphs (bottom) of LTP in control and interleaved Stx-3 Rep CA1 pyramidal cells. Right panel shows scatter plots of individual experiments with mean ± SEM.
Scale bar in all panels represents 20 μm unless otherwise indicated. Calibration bars for sample EPSC traces represent 30 ms and 50 pA. In all panels, each bar represents mean ± SEM (*$p < 0.05$). See also Figures S1 and S2.

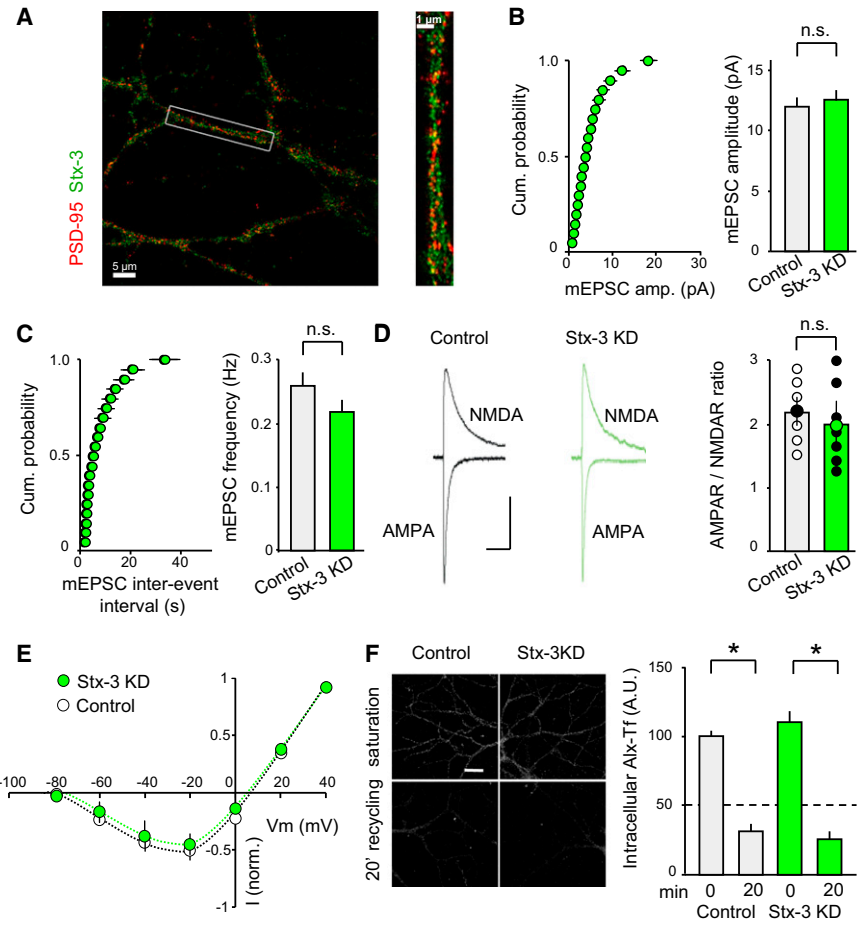

Figure 2. Postsynaptic Stx-3 KD In Vivo Does Not Alter Basal Synaptic Transmission or Constitutive Recycling

(A) Merged images of dendrites stained for endogenous Stx-3 and PSD-95. Right panel shows enlargement of single dendrite (box in left panel). See also Movie S1.

(B and C) Mean amplitude (B) and frequency (C) of mEPSCs are unchanged by the Stx-3 KD. Cumulative probability graphs of mEPSC amplitudes and frequencies are shown on left and summary graphs (means ± SEM) on the right.

(D) The ratio of AMPAR- to NMDAR-mediated EPSCs is unchanged by the Stx-3 KD. Representative EPSCs recorded at −60 mV and +40 mV are shown with scatter plots of individual recordings. Different colored points indicated mean ± SEM. Scale bar represents 50 ms/25 pA.

(E) Voltage dependence of NMDAR EPSCs is not affected by Stx-3 KD.

(F) Representative images and summary graphs showing endosome recycling. Alexa 488-transferrin (Alx-Tf) uptake at time = 0 and after 20 min recycling was measured in control and Stx-3 KD cultured neurons. Loss of Alx-Tf reflects recycling. Bar graphs represent means ± SEM. See also Figure S3.

A critical question about the postsynaptic role of Stx-3 is whether it is exclusively required for LTP or also plays a role in maintaining basal excitatory synaptic transmission. To address this issue, we examined the effect of Stx-3 KD on miniature AMPAR-mediated EPSCs. Neither mEPSC amplitude nor its frequency were affected by the Stx-3 KD (Figure 2B; control amplitude, 11.5 ± 0.7 pA, n = 9; Stx-3 KD 12.0 ± 0.7 pA, n = 8; Figure 2C; control frequency, 0.27 ± 0.02 Hz, Stx-3 KD, 0.22 ± 0.02 Hz). These results suggest that basal AMPAR-mediated synaptic transmission and therefore basal AMPAR trafficking is not affected by postsynaptic Stx-3 KD. To determine whether the postsynaptic Stx-3 KD influenced basal NMDAR-mediated synaptic transmission, we calculated the ratio of AMPAR- to NMDAR-mediated EPSCs (Kauer and Malenka, 2007). This ratio was also not affected by the Stx-3 KD (Figure 2D: control, 2.20 ± 0.18, n = 6; Stx-3 KD, 2.0 ± 0.2, n = 7). Furthermore, the voltage dependence of NMDAR EPSCs (Figure 2E: control, n = 5; Stx-3 KD, n = 5) and their decay time course, which is influenced by the subunit stoichiometry of NMDARs, were not altered by the Stx-3 KD (Figure S3A). Consistent with the Stx-3 KD occurring only postsynaptically at the synapses being studied, Stx-3 KD had no effect on paired-pulse ratios, a measure of changes in presynaptic function (Figure S3B).

The intracellular pool of AMPARs that undergo exocytosis during LTP has been proposed to reside in recycling endosomes (REs) that also contain transferrin receptors (TfRs) (Park et al., 2004; Petrini et al., 2009). REs, however, can give rise to multiple types of exocytic vesicles that are trafficked by distinct pathways (Puthenveedu et al., 2010; Temkin et al., 2011). To determine whether postsynaptic Stx-3 is specifically required for AMPARs exocytosis during LTP or rather globally involved in constitutive trafficking of REs, we examined the endocytic recycling of TfRs in hippocampal neurons. Hippocampal neurons exhibited robust uptake of fluorescent Alexa-Tf into recycling endosomes at steady state (Figure 2F: control, 100.0 ± 5.4 A.U., n = 20; Stx-3 KD, 107.2 ± 8.5 A.U., n = 20). A subsequent 20 min period of incubation in excess unlabeled Tf revealed a loss of intracellular Alexa-Tf, reflecting ongoing basal recycling. This recycling was unaffected by the Stx-3 KD (Figure 2F: control/20 min, 30.7 ± 4.0 A.U., n = 20; Stx-3 KD/20 min, 24.5 ± 2.4 A.U., n = 20). Taken together, these results suggest that postsynaptic Stx-3 is not required for the maintenance of constitutive RE and TfR trafficking or basal AMPAR- or NMDAR-mediated synaptic responses.

Complexin Binding Sequence of Syntaxin-3 Is Required for LTP

The molecular replacement strategy allowed us to perform a detailed structure/function analysis to identify the key molecular sequences of Stx-3 that are required for LTP. We first examined the importance of the Stx-3 complexin binding sequence in

the SNARE motif (aa 213–224) by replacing it with the homologous stretch of amino acids in Stx-4 that do not interact with complexin (Stx-3/4) (Figure 3A). In contrast to wild-type Stx-3 (Figures 1N and 1O), the Stx-3/4 chimera was unable to rescue the increases in GluA1 surface expression triggered by glycine in cultured Stx-3 KD neurons (Figure 3B: control, 100.0% ± 8.0%, n = 24; control/glycine, 230.0% ± 11.4%, n = 24; Stx-3/4, 152.0% ± 5.7%, n = 24; Stx-3/4/glycine, 146.5% ± 11.4%, n = 25) or LTP measured in acute slices after in vivo postsynaptic Stx-3 KD (Figure 3C: control 264.0% ± 18.0%, n = 5; Stx-3/4 127.0% ± 20.0%, n = 6). To further test the importance of the Stx-3 complexin binding sequence, we placed this sequence into Stx-4 by replacing the homologous Stx-4 sequence that does not bind complexin (Stx-4/3) (Pabst et al., 2000). When expressed with the Stx-3 KD, the Stx-4/3 chimera rescued the glycine-induced "LTP" in culture (Figure 3E: control, 100.0% ± 12.0%, n = 24; control/glycine, 230.0% ± 11.4%, n = 24; Stx-4/3, 105.0% ± 12.1%, n = 24; Stx-4/3/glycine, 208.0% ± 15.6%, n = 24) as well as LTP in acute slices (Figure 3F: control, 237.0% ± 25.0%, n = 6; Stx-4/3, 235.0% ± 25.0%, n = 6). Importantly, the replacement of Stx-3 with wild-type Stx-4 (Stx-4 Rep) was unable to rescue the block of glycine-induced increases in GluA1 surface expression in Stx-3 KD cultured neurons (Figures 3G and 3H: control, 100.0% ± 12.0%, n = 24; control/glycine, 230.0% ± 11.4%, n = 24; Stx-4 Rep, 105.0% ± 14.1%, n = 24; Stx-4 Rep/glycine, 100.0% ± 14.3%, n = 24). Similarly, Stx-4 Rep did not rescue LTP induced in CA1 pyramidal cells in acute slices (Figure 3I: control, 250.0% ± 17.0%, n = 6; Stx-4 Rep, 135.0% ± 28.0%, n = 6). These findings are consistent with the requirement for complexin in LTP (Ahmad et al., 2012) and provide strong evidence that complexin binding to Stx-3 is critical for AMPAR delivery during LTP. Notably, cultured neurons expressing the Stx-3/4 chimera exhibited an increase in surface GluA1 levels. Analysis of the mEPSC amplitude and frequency in these neurons revealed that the observed change of surface levels of GluA1 did not correspond to increased excitatory synaptic transmission (Figure S4A). Furthermore, replacement of Stx-3 with the Stx-3/4 chimera in vivo also did not affect mEPSCs recorded from CA1 pyramidal cells in acute slices (Figure S4B). These results suggest the possibility that when freed from complexin regulation, Stx-3 may participate in constitutive AMPARs exocytosis to extrasynaptic sites.

In a final set of experiments on Stx-3, we deleted its amino terminal 8 amino acids (Stx-3^{10-287}) that mediate the binding of syntaxins to Munc18-like proteins (Figure 3J), an interaction that is thought to be critical for catalyzing fusion (Khvotchev et al., 2007; Shen et al., 2007; Südhof and Rothman, 2009). Consistent with this hypothesis, deletion of the N-terminal Munc18-binding peptide ("N-peptide") from Stx-3 abolished the ability of Stx-3 to rescue glycine-induced "LTP" in Stx-3 KD cultured neurons (Figure 3K: control, 100.0% ± 6.0%, n = 22; control/glycine, 217.0% ± 11.4%, n = 22; Stx-3^{10-287}, 91.0% ± 11.9%, n = 22; Stx-3^{10-287}/glycine, 123.0% ± 19.3%, n = 22) and LTP measured in acute slices (Figure 3L: control, 250.0% ± 17.0%, n = 6; Stx-3^{10-287}, 145.0% ± 29.0%, n = 5). Thus, similar to presynaptic exocytosis, a postsynaptic Munc18-like protein is likely required to catalyze the fusion that mediates regulated AMPAR exocytosis during LTP.

Postsynaptic SNAP-25 Regulates Surface NMDAR Levels

In addition to requiring syntaxins, membrane fusion during exocytosis requires the participation of SNARE proteins related to SNAP-25. Four isoforms of this family exist and are expressed in brain (SNAP-23, SNAP-25, SNAP-29, and SNAP-47). To determine which of these isoforms is critical for the activity-dependent trafficking of AMPARs during LTP, we again generated effective and specific shRNAs to each of these proteins, although we were unable to generate an effective shRNA for SNAP-29 (Figure S1). The SNAP-23 KD (Figure 4A) did not alter the glycine-induced increase in GluA1 surface levels (Figure 4B: control, 102.0% ± 4.2%, n = 35; control/glycine 253.0% ± 16.0%, n = 35; SNAP-23 KD, 109.0% ± 5.6%, n = 35; SNAP-23 KD/glycine 247.0% ± 12.3%, n = 35) or LTP generated in acute slices (Figure 4C: control 270.0% ± 15.0%, n = 8; SNAP-23 KD 250.0% ± 15.0%, n = 8). In contrast, the SNAP-25 KD (Figure 4D) prevented the glycine-induced "LTP" in cultured neurons (Figure 4E: control, 102.0% ± 4.2%, n = 35; control/glycine, 253.0% ± 16.0%, n = 35; SNAP-25 KD, 130.0% ± 7.4%, n = 35; SNAP-25 KD/glycine, 131.0% ± 7.5%, n = 35) and strongly impaired the generation of LTP in CA1 pyramidal cells in acute slices (Figure 4F: control, 248.0% ± 14.0%, n = 7; SNAP-25 KD 130.0% ± 16.0%, n = 9). Note that the same SNAP-25 KD, although highly efficient, does not detectably impair presynaptic neurotransmitter release, probably because the presynaptic SNAP-25 concentrations far exceed the needs of the presynaptic release machinery (Sharma et al., 2011). Because postsynaptic SNAP-25 may be critical for NMDAR trafficking (Lau et al., 2010), we explored the possibility that the SNAP-25 KD impaired LTP by reducing the surface levels of NMDARs. Consistent with this hypothesis (Lau et al., 2010), immunostaining for GluN1, a subunit essential for NMDAR function, revealed greatly reduced levels of NMDARs in the dendrites of SNAP-25 KD cells (Figure 4G: control, 100.0% ± 5.7%, n = 46; SNAP-25 KD 55.6% ± 2.2%, n = 46). Furthermore, AMPAR/NMDAR ratios in SNAP-25 KD CA1 pyramidal cells in acute slices were significantly higher than in control cells (Figure 4H: control, 2.3 ± 0.2, n = 6; SNAP-25, KD 3.8 ± 0.2, n = 6).

To determine whether the decrease of synaptic NMDARs due to the SNAP-25 KD could account for the observed impairment in LTP, we elicited LTP in slices preincubated with a concentration of D-APV (10 μM) that reduced NMDAR EPSCs to an extent (~55%; Figure S5A) that is approximately the same as that caused by SNAP-25 KD, as determined by its effects on the AMPAR/NMDAR ratio. LTP was significantly impaired, and almost completely blocked, by this modest concentration of D-APV (Figures S5B and S5C). This result suggests that the impairment of LTP due to the postsynaptic SNAP-25 KD is the result of a deficit in LTP induction caused by a decrease in NMDAR-mediated synaptic currents. Finally, as expected from the purely postsynaptic manipulation of SNAP-25, the SNAP-25 KD in CA1 pyramidal cells had no effect on the paired-pulse ratios of EPSCs (Figure 4I: control, n = 7; SNAP-25 KD, n = 6).

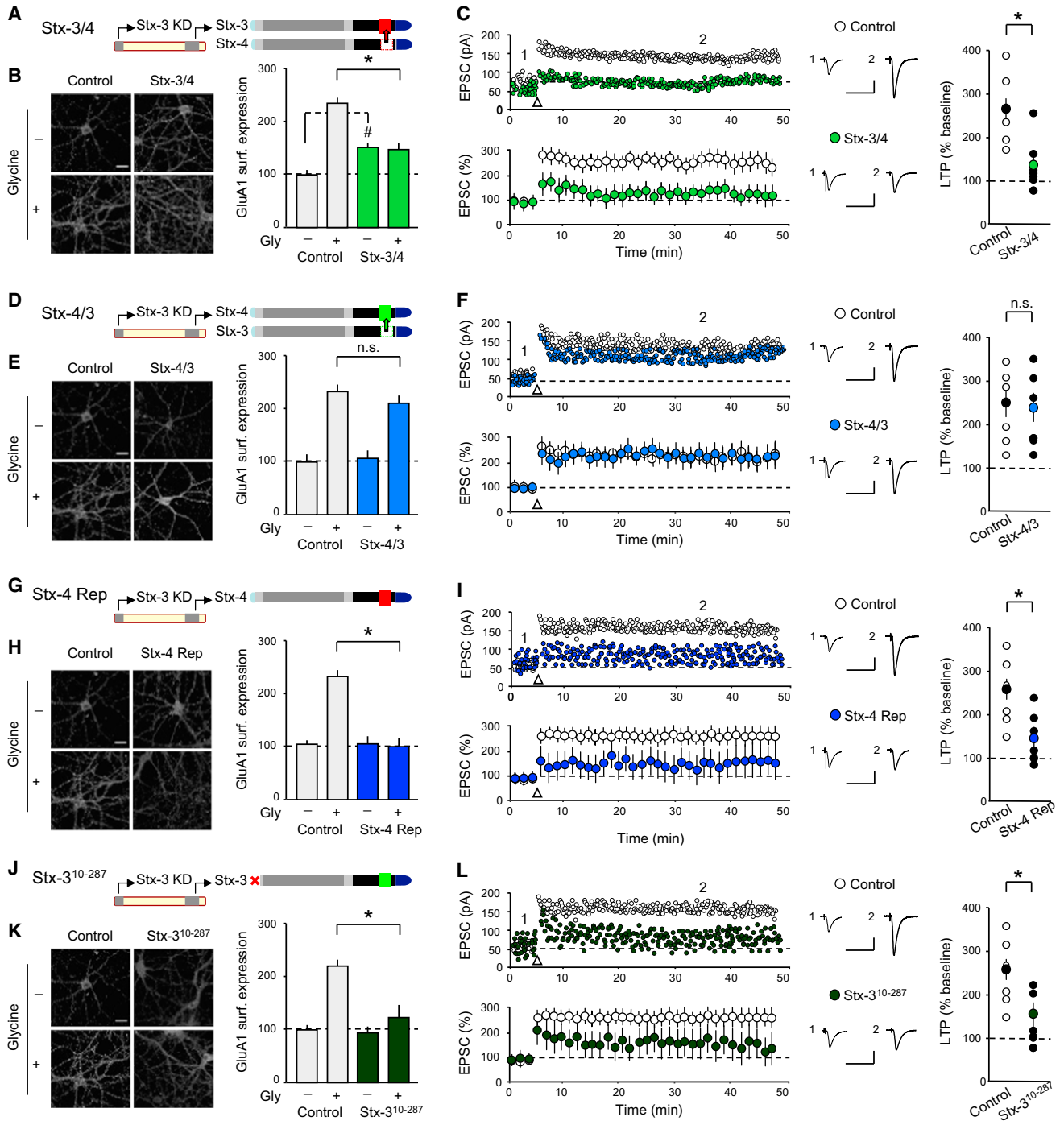

Figure 3. Binding of Complexin to Stx-3 Is Required for LTP

(A) Schematic showing swap of non-complexin binding sequence of Stx-4 into Stx-3.

(B) Sample images and summary graph of glycine-induced changes in surface GluA1 in control neurons and neurons in which the Stx-3/4 chimera replaced Stx-3.

(C) Sample experiments (top) and summary graphs (bottom) of LTP in control and Stx-3/4 CA1 pyramidal cells. Right panel shows scatter plots of individual experiments with mean ± SEM.

(D) Schematic showing swap of complexin binding sequence of Stx-3 into Stx-4.

(E) Sample images and summary graph of glycine-induced changes in surface GluA1 in control and Stx-4/3 cultured neurons.

(F) Sample experiments (top) and summary graphs (bottom) of LTP in control and Stx-4/3 CA1 pyramidal cells. Right panel shows scatter plots of individual experiments with mean ± SEM.

(G) Schematic showing Stx-4 replacement.

(legend continued on next page)

Postsynaptic SNAP-47 Is Required for AMPAR Delivery during LTP

We next examined the role of SNAP-47, which is detected at high levels in brain (see Allen Brain Atlas and Figure S1B; Holt et al., 2006) and shows a localization distinct from that of typical synaptic vesicle markers such as synapsin or synaptophysin (Holt et al., 2006). SNAP-47 contains a longer N terminus than SNAP-23 or SNAP-25 and includes an extended linker between the two SNARE motifs that lacks palmitoylated cysteine residues (Figure 5A). The SNAP-47 KD prevented the glycine-induced increase in surface GluA1 levels in cultured neurons (Figure 5B: control, 102.0% ± 4.2%, n = 35; control/glycine, 253.0% ± 16.0%, n = 35; SNAP-47 KD, 134.0% ± 7.2%, n = 35; SNAP-47 KD/glycine, 124.0% ± 6.4%, n = 35) and impaired LTP in acute hippocampal slices (Figure 5C: control, 260.0% ± 18.0%, n = 7; SNAP-47 KD, 147.0% ± 19.0%, n = 8). These deficits were fully rescued by simultaneous expression of shRNA-resistant wild-type SNAP-47 (SNAP-47 Rep) (Figure 5D) both in cultured neurons (Figure 5E: control, 100.0% ± 5.0%, n = 32; control/glycine, 218.0% ± 11.4%, n = 34; SNAP-47 Rep, 107.0% ± 7.4%, n = 31; SNAP-47 Rep/glycine, 209.0% ± 8.6%, n = 37) and in vivo in CA1 pyramidal cells (Figure 5F: 250.0%± 19.0%, n = 11; SNAP-47 Rep, 245.0% ± 20.0%, n = 9). Similar to the distribution of Stx-3, structured illumination microscopy revealed that endogenous SNAP-47 was distributed throughout the soma and dendrites and was often found adjacent to PSD-95 puncta (Figure 5G; Movie S2).

To test whether SNAP-47 is required for maintaining basal AMPAR- or NMDAR-mediated synaptic transmission in addition to its role in LTP, we analyzed the effects of the SNAP-47 KD on mEPSCs recorded from CA1 pyramidal cells in acute slices. The SNAP-47 KD had no effect on either the mEPSC amplitude (Figure 5H: control, 10.9 ± 0.4 pA, n = 5; SNAP-47 KD, 11.8 ± 0.6 pA, n = 7) or frequency (Figure 5I: control, 0.26 ± 0.02 Hz; SNAP-47 KD, 0.27 ± 0.02 Hz). Assays of AMPAR/NMDAR ratios (Figure 5J: control, 2.1 ± 0.2, n = 7; SNAP-47 KD, 2.2 ± 0.1, n = 7), the current-voltage relationships of NMDAR EPSCs (Figure 5K: control, n = 5; SNAP-47 KD, n = 6) and the decay time constants of NMDAR EPSCs (Figure S6A) revealed that unlike the SNAP-25 KD, the postsynaptic SNAP-47 KD had no effect on basal NMDAR-mediated synaptic transmission. Furthermore, presynaptic function as assessed by paired-pulse ratios was unaffected (Figure S6B). Similar to the Stx-3 KD, the SNAP-47 KD also did not affect constitutive TfR recycling in cultured neurons (Figure 5L: control, 100.0 ± 5.4 A.U., n = 20; control/20 min, 30.7 ± 4.0 A.U., n = 20; SNAP-47 KD, 92.5 ± 8.8 A.U., n = 20; SNAP-47 KD/20 min, 23.4 ± 2.3 A.U., n = 20). These findings suggest that SNAP-47 specifically participates in the fusion machinery that is responsible for AMPAR exocytosis during LTP.

To determine whether SNAP-47's role in LTP does in fact require its interaction with other SNARE proteins in the formation of SNARE complexes, we deleted the C-terminal 20 amino acids of SNAP-47, a mutation that mimics the effect of botulinum toxin E on SNAP-25 (SNAP-47$^{\Delta Ct}$) (Figure 6A). In SNAP-25, this truncation impairs SNARE complex stability and blocks exocytosis (Blasi et al., 1993). SNAP-47$^{\Delta Ct}$ was unable to rescue the effects of the SNAP-47 KD on the glycine-induced increase in GluA1 surface expression (Figure 6B: control, 100.0% ± 6.0%, n = 22; control/glycine, 217.0% ± 11.4%, n = 22; SNAP-47$^{\Delta Ct}$, 106.0% ± 17.1%, n = 22; SNAP-47$^{\Delta Ct}$/glycine, 114.0% ± 11.2%, n = 22). Similarly, SNAP-47$^{\Delta Ct}$ did not rescue LTP induced in SNAP-47 deficient CA1 pyramidal cells in acute slices (Figure 6C: control, 255.0% ± 20.0%, n = 6; SNAP-47$^{\Delta Ct}$, 130.0% ± 30.0%, n = 7). In contrast, replacing the extended amino-terminus of SNAP-47 with the shorter sequence of SNAP-25 (SNAP-47^{25Nt}) (Figure 6D), did not affect the rescue of the impairment of glycine-induced increases in GluA1 surface expression caused by the SNAP-47 KD (Figure 6E: control, 100.0% ± 6.0%, n = 22; control/glycine, 217.0% ± 11.4%, n = 22; SNAP-47^{25Nt}, 109.0% ± 7.1%, n = 22; SNAP-47^{25Nt}/glycine, 190.0% ± 13.2%, n = 22) or the rescue of LTP examined in acute slices (Figure 6F: control, 230.0% ± 25.0%, n = 6; SNAP-47^{25Nt}, 210.0% ± 28.0%, n = 6). These findings suggest that the interaction of SNAP-47 with other SNARE proteins to form SNARE complexes is critical for its role in LTP but that its extended N terminus is not.

Synaptobrevin-2 Is Required for Delivery of AMPARs to the Plasma Membrane

Previous studies using intracellular loading of botulinum toxin B, which cleaves synaptobrevin-2 (Schiavo et al., 1992), into CA1 pyramidal cells suggested that this protein is the critical R-SNARE for the delivery of AMPARs to the plasma membrane during LTP (Lledo et al., 1998). Consistent with this hypothesis, the glycine-induced increase in GluA1 surface expression was absent in cultured neurons prepared from synaptobrevin-2 knockout mice (Schoch et al., 2001) (Figure 7A: control, 100.0% ± 8.4%, n = 26; control/glycine, 260.0% ± 12.4%, n = 26; Syb-2 KO, 47.9% ± 6.7%, n = 26; Syb-2 KO/glycine, 54.0% ± 5.7%, n = 26). Given that mEPSC amplitudes were previously found to be unaffected in cultured neurons from these mice (Schoch et al., 2001), it was surprising to find that basal surface GluA1 levels in cultured neurons lacking synaptobrevin-2 were significantly decreased. Because homozygous synaptobrevin-2 knockout mice die at birth (Schoch et al., 2001), we were unable to perform electrophysiological recordings in acute hippocampal slices. Instead, we recorded mEPSCs from wild-type and synaptobrevin-2 knockout cultured neurons and confirmed the

(H) Sample images and summary graph of glycine-induced changes in surface GluA1 in control neurons and neurons in which Stx-4 replaced Stx-3.
(I) Sample experiments (top) and summary graphs (bottom) of LTP in control and Stx-4 Rep CA1 pyramidal cells. Right panel shows scatter plots of individual experiments with mean ± SEM.
(J) Schematic showing mutant form of Stx-3$^{10\text{-}287}$, in which the first 10 amino acids of Stx-3 are deleted, as the replacement construct in Stx-3 KD cells.
(K) Sample images and summary graph of glycine-induced changes in surface GluA1 in control cultured neurons and neurons in which Stx-3$^{10\text{-}287}$ replaced Stx-3.
(L) Sample experiments (top) and summary graphs (bottom) of LTP in control and Stx-3$^{10\text{-}287}$ CA1 pyramidal cells. Right panel shows scatter plots of individual experiments with mean ± SEM.
Scale bars in all images represent 20 μm. Calibration bars represent 30 ms and 50 pA. Bar graphs represent means ± SEM. *p < 0.05. See also Figure S4.

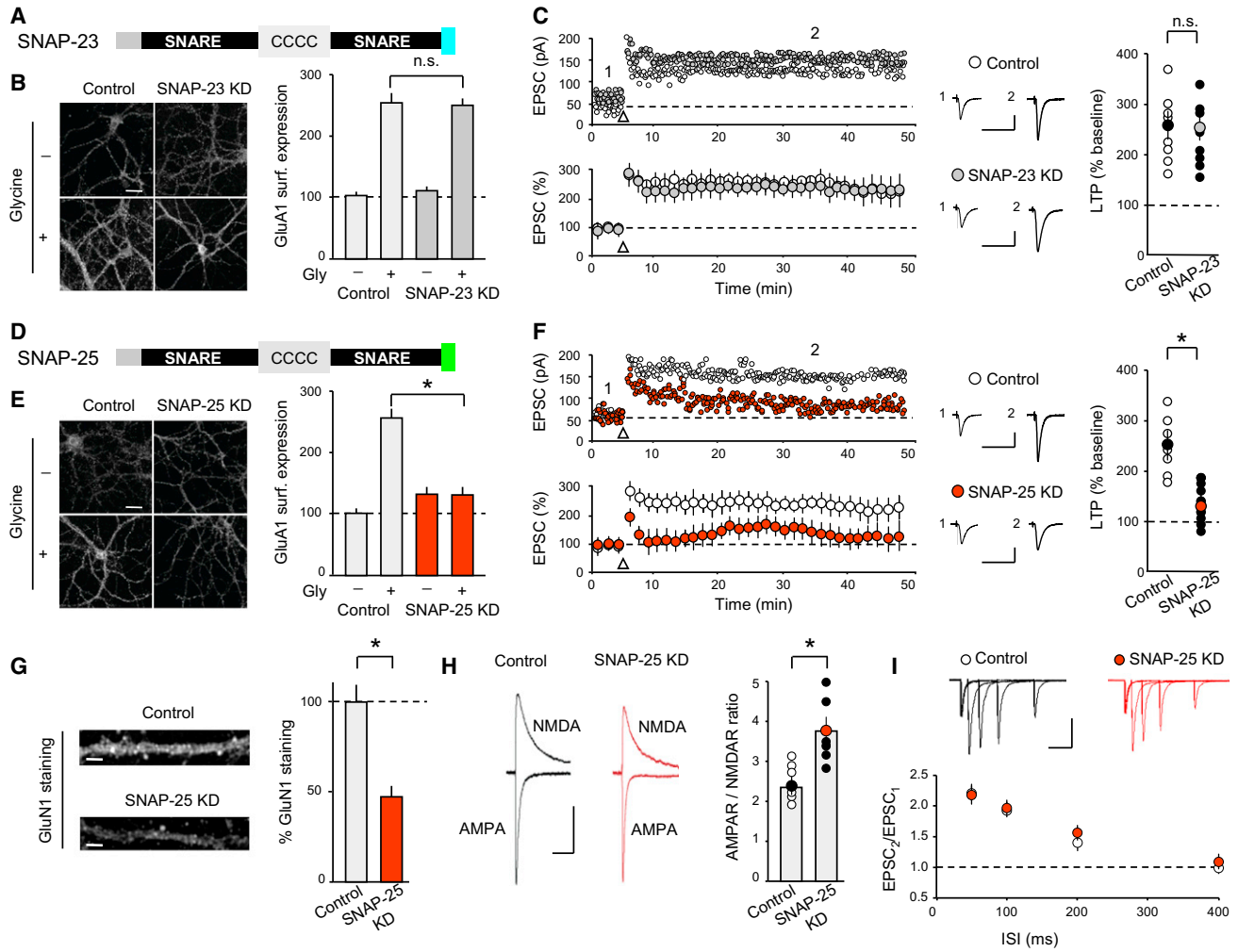

Figure 4. Postsynaptic SNAP-25 KD Impairs LTP and NMDAR-Mediated Transmission

(A) Schematic of SNAP-23 showing its functional domains. C indicates palmitoylated cysteine residues. The colored C terminus represents amino acids cleaved by botulinum toxin E.

(B) Sample images and summary graph of glycine-induced changes in surface GluA1 in control and SNAP-23 KD neurons.

(C) Sample experiments (top) and summary graphs (bottom) of LTP in control and SNAP-23 KD CA1 pyramidal cells. Right panel shows scatter plots of individual experiments with mean ± SEM.

(D) Schematic of SNAP-25. Sequence of amino acids cleaved by botulinum toxin E differs from that in SNAP-23 (in green).

(E) Sample images and summary graph of glycine-induced changes in surface GluA1 in control and SNAP-25 KD neurons.

(F) Sample experiments (top) and summary graphs (bottom) of LTP in control and SNAP-25 KD CA1 pyramidal cells. Right panel shows scatter plots of individual experiments with mean ± SEM.

(G) Sample images of dendritic GluN1 staining. Bar graph shows total GluN1 staining normalized to control cells. Scale bar represents 10 μm.

(H) Ratio of AMPAR- to NMDAR-mediated EPSCs is increased in SNAP-25 KD cells. Representative EPSCs recorded at −60 mV and + 40 mV are shown (mean ± SEM is indicated by symbol with different color). Calibration bars represent 50 ms and 25 pA.

(I) Paired-pulse ratios of AMPAR EPSCs are unchanged by postsynaptic SNAP-25 KD. Representative EPSCs are shown above summary graph. Calibration bars represent 100 ms/100 pA.

Scale bars in (B)–(E) represent 20 μm. Calibration bars in (C) and (F) represent 30 ms/50 pA. Bar graphs represent means ± SEM. *$p < 0.05$. See also Figure S5.

immunocytochemical results as well as previous results (Schoch et al., 2001). Glycine treatment increased the mEPSC amplitude in control cultured neurons but not in cultured neurons lacking synaptobrevin-2, while having no effect on basal mEPSC amplitude (Figure 7B: control, 16.8 ± 0.7 pA, n = 17; control/glycine, 24.1 ± 0.6 pA, n = 16; Syb-2 KO, 17.1 ± 0.7 pA, n = 8; Syb-2 KO/glycine, 16.7 ± 0.7 pA, n = 8). As expected from the presynaptic functions of synpatobrevin-2, the mEPSC frequency was dramatically reduced in the synaptobrevin-2 knockout cultures and was not increased by glycine treatment (Figure 7C: control, 6.8 ± 0.3 Hz; control/glycine, 12.7 ± 0.3 Hz; Syb-2 KO, 1.70 ± 0.2 Hz, Syb-2 KO/glycine,1.8 ± 0.2 Hz).

To directly test that the postsynaptic deficits in the synaptobrevin-2 knockout cultures were in fact due to the loss of

synaptobrevin-2, we performed rescue experiments in which we expressed wild-type synaptobrevin-2 in cultured synaptobrevin-2 knockout neurons using lentiviruses. Expression of synaptobrevin-2 rescued both the reduction in basal surface GluA1 levels in cultured synaptobrevin-2 knockout neurons as well as the loss of glycine-induced "LTP" (Figure 7D: control, 100.0% ± 4.8%, n = 20; Syb-2 Res, 98.7% ± 7.9%, n = 16; control/glycine, 176.4% ± 9.5%, n = 20; Syb-2 Res/glycine, 189.2% ± 10.7%, n = 20). Furthermore, synaptobrevin-2 rescued neurons showed a mEPSC frequency comparable to control cells and a substantial increase in both the mEPSC amplitude and frequency in response to glycine (Figure 7E: amplitude—control, 16.8 ± 0.7 pA, n = 17; control/glycine, 24.1 ± 0.6 pA, n = 16; Syb-2 Res, 17.3 ± 1.2 pA, n = 12; Syb-2 Res/glycine, 22.5 ± 0.9 pA, n = 10; Figure 7F: frequency—control, 6.8 ± 0.3 Hz; control/glycine, 12.7 ± 0.3 Hz; Syb-2 Res, 5.7 ± 0.8 Hz, Syb-2 Res/glycine,10.4 ± 0.7 Hz). Notably, synaptobrevin-2 knockout neurons exhibited an impairment in constitutive TfR recycling (Figure 7G: control, 100.0 ± 4.7 A.U., n = 20; control/20 min, 50.0 ± 3.4 A.U., n = 20; Syb-2 KO, 100.0 ± 6.55 A.U., n = 20; Syb-2 KO/20 min, 80.0 ± 4.9 A.U., n = 20), which was rescued by expression of wild-type synaptobrevin-2 (Figure 7H: control bars are the same as Figure 7G; Syb-2 Res, 100.0 ± 5.6 A.U., n = 20; Syb-2 Res/20 min, 40.3 ± 6.7 A.U., n = 20). These findings suggest that synpatobrevin-2 is involved in both the constitutive delivery of AMPARs to the plasma membrane as well as the enhanced regulated delivery of AMPARs during LTP, but is absolutely required only for the latter.

DISCUSSION

The molecular mechanisms underlying the SNARE-dependent fusion of neurotransmitter-containing vesicles with the presynaptic plasma membrane at the active zone have been studied for decades and are well understood (Rizo and Rosenmund, 2008; Südhof, 2004; Südhof and Rothman, 2009). In contrast, although postsynaptic exocytosis in dendrites may mediate important neuronal functions including the regulated membrane insertion of AMPARs during LTP (Kennedy et al., 2010; Kennedy and Ehlers, 2011; Lledo et al., 1998; Lüscher et al., 1999; Makino and Malinow, 2009), the composition of postsynaptic SNARE complexes mediating AMPAR exocytosis in dendrites remains unknown. Using a molecular replacement strategy that allows the postsynaptic targeting of molecular manipulations in vivo as well as identical molecular manipulations in vitro, we have identified the composition of the SNARE complex that mediates the regulated delivery of AMPARs to the plasma membrane during LTP. Specifically, we provide evidence that the Q-SNARE proteins Stx-3 and SNAP-47 and the R-SNARE protein synaptobrevin-2 are essential components of the postsynaptic vesicle fusion machinery that is required for LTP; the same SNARE proteins are not absolutely required for the constitutive delivery of AMPARs and NMDARs to synapses (Figure 8). Moreover, our data indicate that synaptobrevin-2 contributes to constitutive postsynaptic AMPAR trafficking, and support the notion that SNAP-25 plays a role in the constitutive postsynaptic trafficking of NMDARs (Lau et al., 2010).

Consistent with the requirement of complexin binding to postsynaptic SNARE complexes during LTP (Ahmad et al., 2012), we show that the role of postsynaptic Stx-3 in LTP depends on its ability to bind to complexin. Although previous work suggested that Stx-4 is critical for AMPAR exocytosis during LTP (Kennedy et al., 2010), we present several lines of evidence suggesting that this is not the case. First, KD of Stx-4 had no effect on glycine-induced GluA1 trafficking in cultured neurons or on LTP measured in acute slices after Stx-4 KD in vivo. Second, while the effects of the Stx-3 KD could be rescued by expression of wild-type Stx-3, expression of wild-type Stx-4 was ineffective unless its sequence that does not bind complexin was replaced by the homologous Stx-3 sequence that confers complexin binding. Furthermore, immunogold labeling of Stx-3 and- 4 reveals that Stx-3 is prominently found in dendritic membranes whereas Stx-4 is more abundant in astroglial plasma membranes (J.H. Tao-Cheng et al., 2012, Soc. Neurosci., abstract).

The difference in conclusions regarding Stx-4 may in large part be due to differences in the assays used. Here, we intentionally measured NMDAR-triggered changes in the levels of surface expression of endogenous AMPARs in cultured neurons and monitored standard LTP in slices from mice subjected to in vivo manipulations. The previous work monitored the role of syntaxins in cultured neurons using the trafficking of recombinant TfRs fused to superecliptic pHluorin (TfR-SEP) as a surrogate marker of the AMPAR trafficking pathways (Kennedy et al., 2010). Measurements of the trafficking of overexpressed TfR-SEP may not accurately reflect the trafficking of endogenous AMPARs since AMPARs may traffic independently of TfRs and overexpressed proteins may traffic aberrantly. Given that individual endosomes can sort different cargos via independent microdomains (Puthenveedu et al., 2010; Temkin et al., 2011), different syntaxin isoforms may coexist in postsynaptic compartments and participate in distinct trafficking pathways. Consistent with this notion, the Stx-3 KD in cultured neurons did not affect constitutive recycling of TfRs or constitutive exocytosis of AMPARs (Figure 2).

Previous work also used acute infusion of a Stx-4 "inhibitory" peptide into CA1 pyramidal cells to disrupt Stx-4 function and reported an impairment of LTP measured electrophysiologically (Kennedy et al., 2010). Although useful, such manipulations may have off-target effects. For example, the promiscuous engagement of SNARE motifs in SNARE complexes once they are freed from their normal cell-biological constraints may have influenced the activity of these peptides (Fasshauer et al., 1999; Yang et al., 1999). It is also plausible that compensatory effects due to long-term knockdown of Stx-3 may account for the impairment in LTP that we observed. However, given that protein levels of Stx-4 were unaltered in Stx-3 KD cells (Figure S1B) and that the expression of recombinant Stx-4 was unable to rescue glycine-induced AMPAR exocytosis or LTP in neurons lacking endogenous Stx-3 (Figures 3H–3I), it appears that Stx-4 cannot compensate for the loss of Stx-3 function in regulated AMPAR trafficking.

The effects of mutations of Stx-3 suggest that it functions postsynaptically in regulating AMPAR delivery to the plasma membrane in a manner analogous to the function of Stx-1 in presynaptic

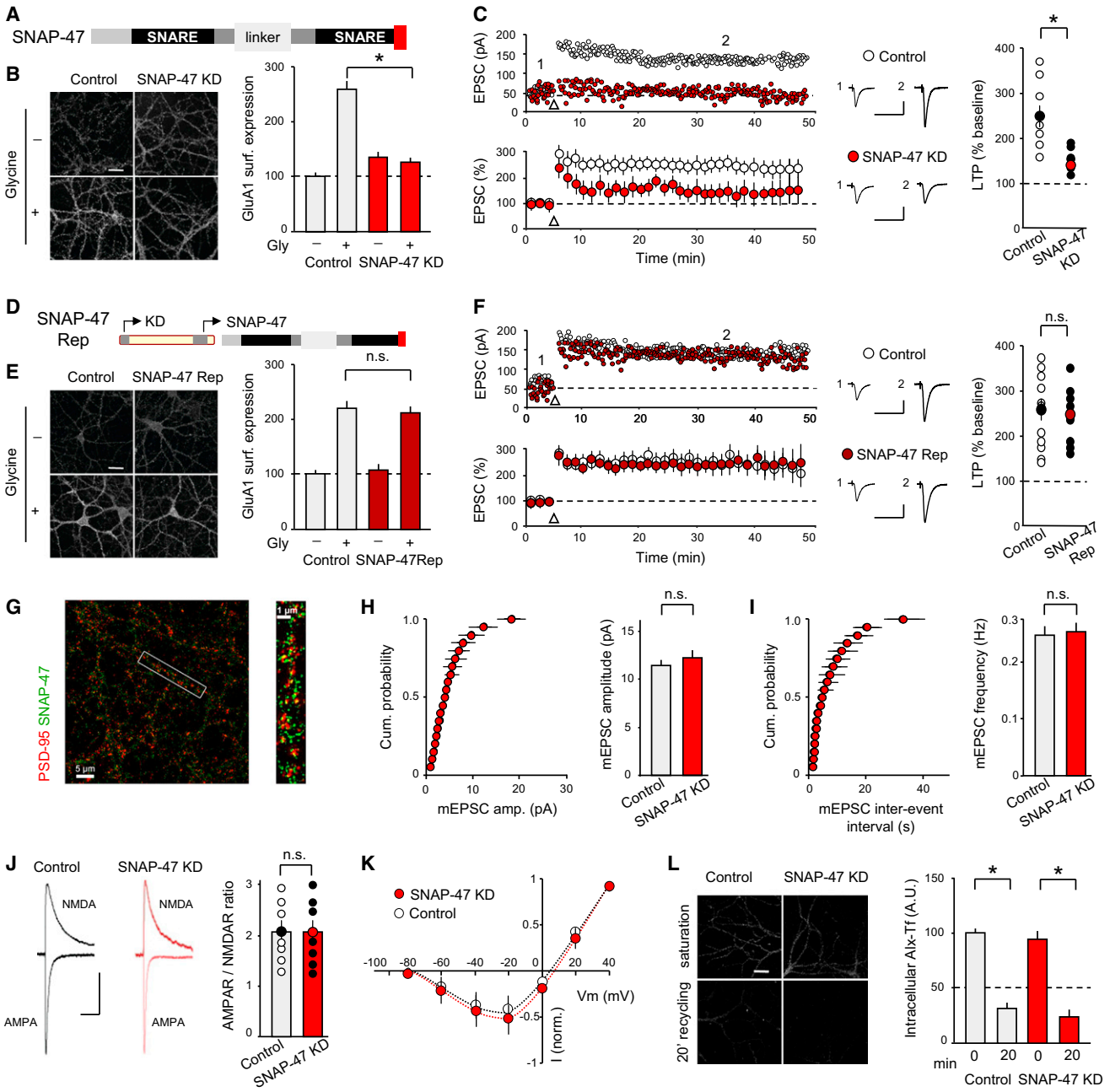

Figure 5. Postsynaptic SNAP-47 KD Impairs LTP without Altering Basal Synaptic Transmission or Constitutive Recycling

(A) Schematic of SNAP-47 showing its main functional domains. Note the elongated N terminus and linker without palmitoylated cysteine residues. Lack of botulinum toxin E cleavage site is indicated in red.

(B) Sample images and summary graph of glycine-induced changes in surface GluA1 in control and SNAP-47 KD neurons.

(C) Sample experiments (top) and summary graphs (bottom) of LTP in control and SNAP-47 KD CA1 pyramidal cells. Right panel shows scatter plots of individual experiments with mean ± SEM.

(D) Schematic showing molecular replacement strategy for SNAP-47.

(E) Sample images and summary graph showing rescue of glycine-induced increases in surface GluA1 by SNAP-47.

(F) Sample experiments (top) and summary graphs (bottom) of LTP in control and interleaved SNAP-47 Rep CA1 pyramidal cells. Right panel shows scatter plots of individual experiments with mean ± SEM.

(G) Merged images of dendrites stained for endogenous SNAP-47 and PSD-95. Right panel shows enlargement of single dendrite (box in left panel). See also Movie S2.

(H and I) Mean amplitude (H) and frequency (I) of mEPSCs are unchanged by postsynaptic SNAP-47 KD. Cumulative probability graphs of mEPSC amplitudes and frequencies are shown on left and summary graphs (means ± SEM) on right.

(legend continued on next page)

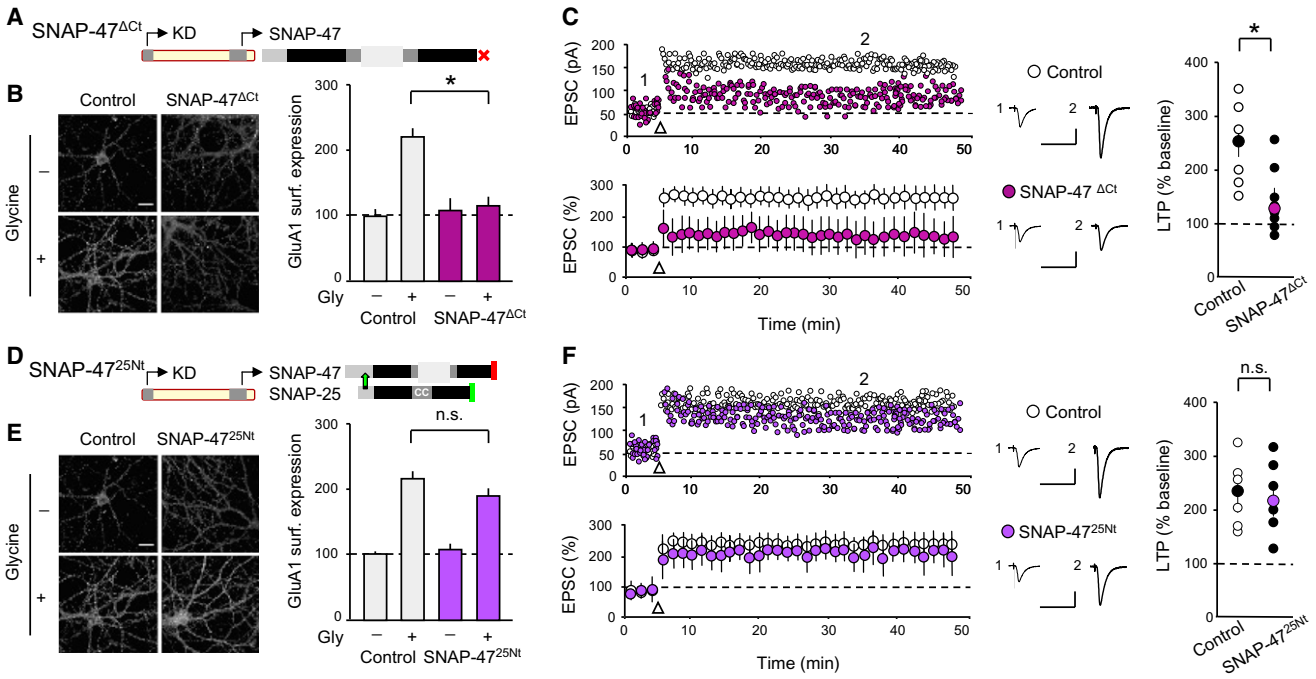

Figure 6. SNARE-Dependent Interaction Is Required for SNAP-47's Role in LTP

(A) Schematic illustrating SNAP-47$^{\Delta Ct}$.

(B) Sample images and summary graph of glycine-induced changes in surface GluA1 in control and SNAP-47$^{\Delta Ct}$ cultured neurons.

(C) Sample experiments (top) and summary graphs (bottom) of LTP in control and SNAP-47$^{\Delta Ct}$ CA1 pyramidal cells. Right panel shows scatter plots of individual experiments with mean ± SEM.

(D) Schematic showing the SNAP-47 N terminus (Nt) swap mutant SNAP-47^{25Nt} in which the Nt of SNAP-47 is replaced by the Nt of SNAP-25.

(E) Sample images and summary graph of glycine-induced changes in surface GluA1 in control and SNAP-47^{25Nt} neurons.

(F) Sample experiments (top) and summary graphs (bottom) of LTP in control and SNAP-47^{25Nt} CA1 pyramidal cells. Right panel shows scatter plots of individual experiments with mean ± SEM.

In (B) and (E), scale bars represent 20 μm. Calibration bars represent 30 ms/50 pA. Bar graphs represent means ± SEM. *$p < 0.05$.

vesicle fusion. Expression of the Stx-3 mutant unable to bind to complexin (Stx-3/4) increased surface expression of GluA1-containing AMPARs but not mEPSC amplitudes, suggesting that extrasynaptic AMPARs were increased. These results imply that postsynaptic complexin binding to syntaxins may constitutively restrict membrane fusion of AMPAR-containing endosomes in a fashion analogous to the role of complexin in clamping presynaptic vesicle fusion (Giraudo et al., 2006; Huntwork and Littleton, 2007; Maximov et al., 2009; Tang et al., 2006: Xue et al., 2009; Yang et al., 2010). Inhibition of the binding of SM proteins to Stx-3 also impaired LTP, a finding consistent with the hypothesis that binding of syntaxins to SM proteins is required to execute fusion in conjunction with the SNARE protein complexes (Khvotchev et al., 2007; Shen et al., 2007; Südhof and Rothman, 2009).

SNARE-mediated membrane fusion during exocytosis requires participation of a SNAP-25 homolog in addition to a syntaxin (Jahn and Scheller, 2006; Rizo and Rosenmund, 2008; Südhof and Rothman, 2009). Consistent with this principle, we found that KD of either SNAP-25 or SNAP-47, but not SNAP-23, impairs LTP in both slices and cultured neurons. The SNAP-25 KD impaired NMDAR-mediated transmission in slices and, in agreement with previous work (Lau et al., 2010), decreased synaptic NMDAR levels in cultured neurons. Since additional experiments strongly suggested that the observed effects on LTP are due to inadequate activation of NMDARs during LTP induction, we did not further pursue the possible postsynaptic role of SNAP-25 in LTP. The KD of SNAP-23, a SNAP-25 homolog also reported to regulate surface levels of NMDARs (Suh et al., 2010) did not have detectable effects in our LTP assays. Because we used strong induction protocols to elicit LTP, it is possible that via effects on NMDAR trafficking, a function of SNAP-23 in setting the threshold for LTP induction

(J) Ratio of AMPAR- to NMDAR-mediated EPSCs is unchanged by postsynaptic SNAP-47 KD. Representative EPSCs recorded at −60 mV and + 40 mV (left). Scatter plots of individual experiments with mean ± SEM (right). Scale bar represents 50 ms/25 pA.

(K) Voltage-dependence of NMDAR EPSCs is not affected by postsynaptic SNAP-47 KD.

(L) Representative images and summary graphs showing endosome recycling. Uptake and 20 min recycling was measured in control and SNAP-47 KD cells. Loss of Alx-Tf reflects recycling.

Calibration bars in (C) and (F) represent 30 ms and 50 pA. Bar graphs represent means ± SEM. *$p < 0.05$. See also Figure S6.

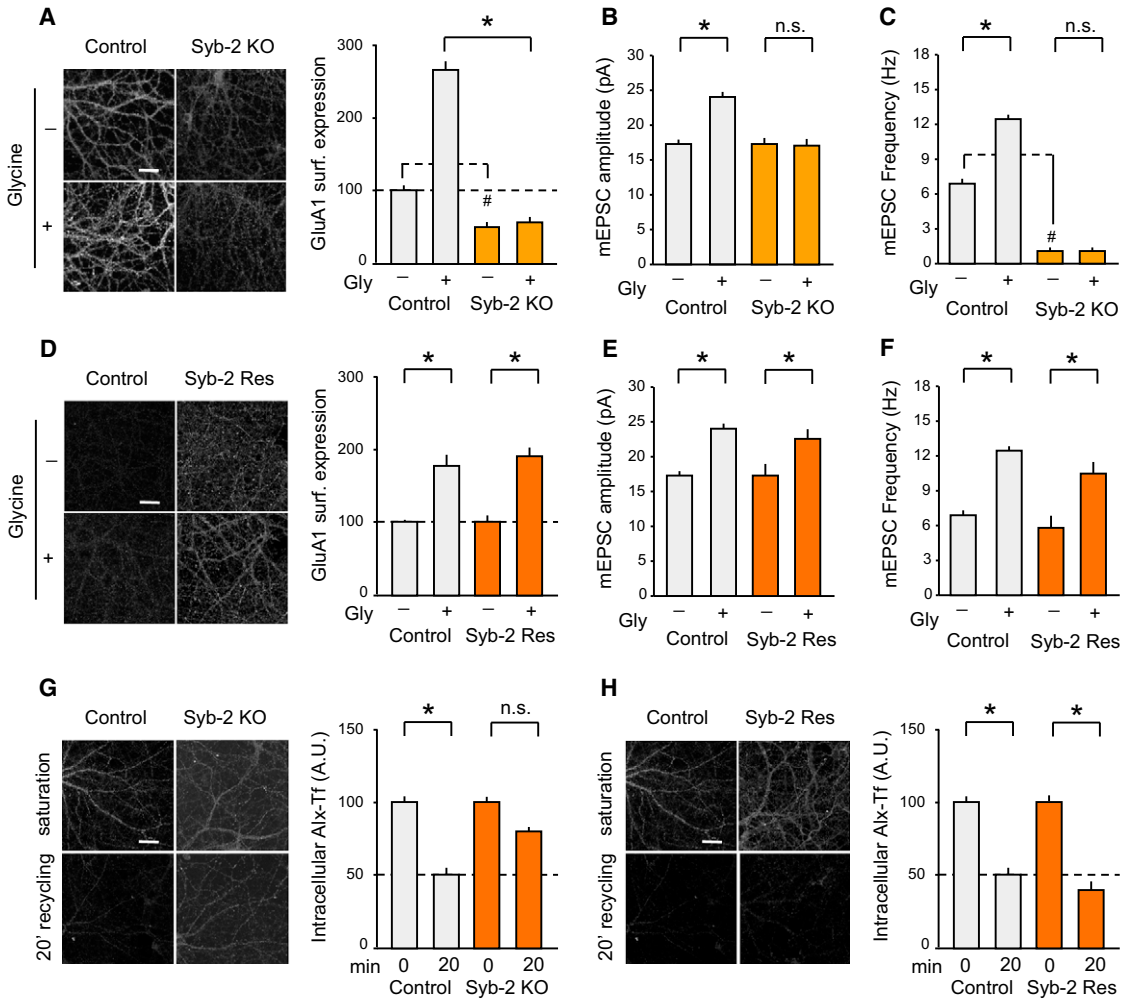

Figure 7. Synaptobrevin-2 Is Required for AMPAR Surface Delivery

(A) Sample images and summary graph of glycine-induced changes in surface GluA1 in control and cultured neurons prepared from Syb-2 KO mice. Scale bars represent 20 μm.

(B and C) Summary graphs of mean mEPSC amplitude and frequency in control and Syb-2 KO cultured neurons before and after glycine application.

(D) Sample images and summary graph of glycine-induced changes in surface GluA1 in control cultured neurons and Syb-2 KO cultured neurons infected with lentivirus expressing Syb-2 (Syb-2 Res). Scale bars represent 20 μm.

(E and F) Summary graphs of mean mEPSC amplitude and frequency in control and Syb-2 Res cultured neurons before and after glycine application.

(G) Images and summary graphs showing endosome recycling. Alx-Tf uptake and 20 min recycling was measured in cultured hippocampal neurons under basal conditions in control and Syb-2 KO cells.

(H) The same as G with Syb-2 rescue (Syb-2 Res). Bar graphs represent means ± SEM. *$p < 0.05$.

went undetected. Arguably the most surprising conclusion from the present study is that postsynaptic SNAP-47, a SNAP-25 homolog that has not been functionally characterized, is critical for LTP. SNAP-47 is found at high levels in the brain and assembles into stable SNARE complexes with Stx-1A and synaptobrevin-2 (Holt et al., 2006). Importantly, the SNAP-47 KD did not alter basal AMPAR- or NMDAR-mediated synaptic responses or basal AMPAR surface expression, providing evidence of a specific role for SNAP-47 in regulated AMPAR exocytosis but not in AMPAR or TfR constitutive trafficking. Moreover, mutagenesis of SNAP-47 confirmed that a SNARE-dependent interaction is critical for its role in LTP.

To complete the characterization of the postsynaptic SNARE complex responsible for regulated AMPAR delivery during LTP, we examined cultures prepared from synaptobrevin-2 KO mice. Our findings confirmed previous work suggesting a role of synaptobrevin-2 in LTP (Lledo et al., 1998) and further demonstrated that synaptobrevin-2 contributes to maintaining extrasynaptic AMPARs. This latter observation raises the question of which SNARE proteins control the constitutive delivery of glutamate receptors to the plasma membrane. The results presented here as well as previous results demonstrating a role for postsynaptic complexin in LTP (Ahmad et al., 2012) suggest that there are two independent pathways for AMPAR delivery; a highly

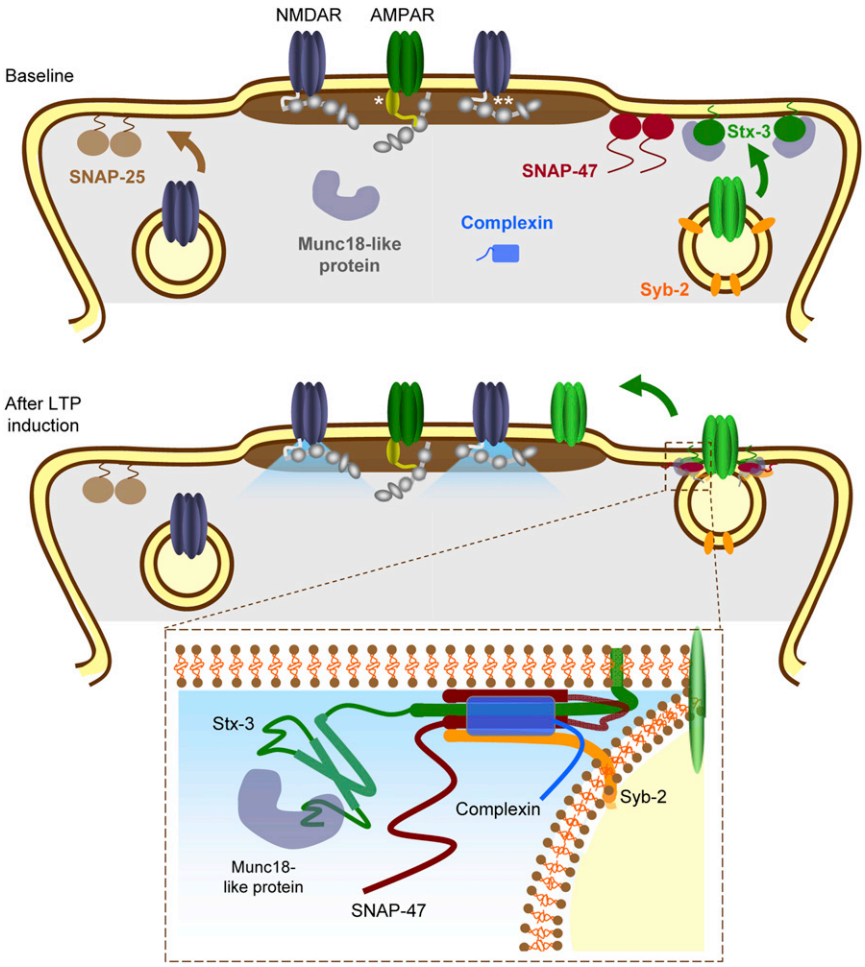

Figure 8. Model of the SNARE Proteins Involved in the Activity-Dependent Exocytosis of AMPARs during LTP

Top panel illustrates different components of the critical SNARE complexes including Stx-3, SNAP-47, and Syb-2. SNAP-25 is shown anchored to the plasma membrane where it influences NMDAR trafficking whereas anchored Stx-3 regulates AMPAR trafficking. * indicates a TARP bound to synaptic AMPARs; ** indicates PSD-95 or another MAGUK family member. Bottom panel: Upon NMDAR activation, calcium influx promotes SNARE-dependent membrane fusion of AMPAR-containing endosomes. Inset panel: the AMPAR exocytosis is mediated by a SNARE complex containing Stx-3, SNAP-47, Syb-2, complexin, as well as a Munc18-like protein.

regulated pathway that is engaged during LTP induction and requires some, as yet unidentified, calcium-regulated protein or step (Figure 8) and a constitutive pathway that delivers these receptors to the plasma membrane (Adesnik et al., 2005). Synaptobrevin-2 may be a component of the AMPAR-containing organelles involved in both pathways, although other R-SNAREs must contribute as well since surface levels of AMPARs were only partly reduced in cells lacking synaptobrevin-2. In contrast, syntaxin-3 and SNAP-47 appear to be exclusively involved in regulated AMPAR exocytosis during LTP.

Our results do not allow any conclusions about the specific dendritic nanodomains at which AMPAR exocytosis occurs during LTP or about the specific timing of these events. These topics have been extensively explored using live cell imaging of overexpressed recombinant proteins fused to fluorophores (i.e., AMPAR subunits or TfR) (Kennedy et al., 2010; Kopec et al., 2006, 2007; Lin et al., 2009; Makino and Malinow, 2009; Opazo et al., 2010; Patterson et al., 2010; Petrini et al., 2009; Tanaka and Hirano, 2012; Yang et al., 2008; Yudowski et al., 2007) with some inconsistency in results, possibly because all of these studies use overexpressed proteins. Most but not all studies find that following NMDAR activation, recombinant AMPAR subunits are inserted into perisynaptic membranes, either adjacent to the PSD or adjacent to the base of dendritic spines, from which they can laterally diffuse into the PSD to increase synaptic strength (Petrini et al., 2009; Opazo et al., 2010). The source of the intracellular AMPARs that are exocytosed during LTP have been suggested to be recycling endosomes containing TfRs (Park et al., 2004). However, our findings, as well as recent work on the complexity of endosome to plasma membrane trafficking (Temkin et al., 2011; Puthenveedu et al., 2010), suggest that more work on this topic is warranted.

Although in this and previous work (Ahmad et al., 2012) we have pointed out several mechanistic similarities between the presynaptic SNARE-mediated exocytosis mediating transmitter release and the postsynaptic SNARE-mediated exocytosis of AMPARs during LTP, there are important differences that may account for the distinct roles of specific SNARE proteins. Presynaptic vesicle exocytosis occurs rapidly (in <1 ms) following a rise in calcium at specialized active zones that provide the critical structural scaffolds mediating this process. In contrast, the intracellular organelles containing dendritic AMPARs are not docked at the plasma membrane but instead may require myosin-dependent trafficking into dendritic spines (Correia et al., 2008; Wang et al., 2008). Indeed, the timing of AMPAR exocytosis following LTP induction may be several orders of magnitude slower than presynaptic vesicle exocytosis (Makino and Malinow, 2009; Patterson et al., 2010; Petrini et al., 2009; Yang et al., 2008; Yudowski et al., 2007), even if myosin-dependent trafficking is not required (Tanaka and Hirano, 2012). However, no direct measurements of endogenous AMPAR exocytosis exist, and its time course is unknown. The differences in the SNARE proteins mediating the two distinct types of pre- and postsynaptic exocytosis at or near synapses likely contribute to their different properties. Furthermore, in contrast to SNAP-23 and SNAP-25, which are predominantly localized to the plasma

membrane, SNAP-47 lacks an immediately identifiable membrane anchor sequence and may be partly soluble (Holt et al., 2006). This biophysical modification might be useful in regulating fusion between membranes where exocytotic domains are not permanent but rather transiently defined (Patterson et al., 2010; Petrini et al., 2009; Yang et al., 2008; Yudowski et al., 2007). By identifying the unique SNARE proteins involved in AMPAR delivery to the plasma membrane during LTP, we have provided information that is critical for a molecular understanding of LTP. More broadly, the findings presented here provide tools and approaches that can be used to further explore the role of LTP in the circuit modifications underlying experience-dependent plasticity.

EXPERIMENTAL PROCEDURES

CD1 (Charles River) mice (8–12 g) were prepared for stereotactic injection of lentiviruses using standard procedures approved by the Stanford University Administrative Panel on Laboratory Animal Care. LTP experiments were performed using whole-cell voltage-clamp recordings from CA1 pyramidal neurons in acute slices as previously described (Ahmad et al., 2012). Dissociated hippocampal cultures were prepared from newborn C57BL/6 mice infected with lentiviruses at DIV 8–9 and processed for experiments 10–11 days later as previously described (Ahmad et al., 2012).

Full Experimental Procedures and any associated references are available in the Supplemental Information.

SUPPLEMENTAL INFORMATION

Supplemental Information includes six figures, two movies, and Supplemental Experimental Procedures and can be found with this article online at http://dx.doi.org/10.1016/j.neuron.2012.11.029.

ACKNOWLEDGMENTS

We thank members of the Malenka and Südhof labs for comments and help during the course of the experiments. We thank Drs. P. Zhou and X. Yang for maintaining the synaptobrevin-2 knockout mouse colony. S.J. performed recordings from acute slices and stereotactic injections. D.G. performed all assays in hippocampal cultures. S.J. and D.G. constructed plasmids, generated lentivirus, and performed western blot analyses. D.G. and A.J.M.M. carried out transferrin recycling assays. Y.Z. designed shRNAs for Stx-3, Stx-4, Stx-1, SNAP-25, SNAP-23, and SNAP-47, generated all KD constructs, and identified effective shRNAs. S.J., D.G., T.C.S., and R.C.M. wrote the manuscript. All authors reviewed the paper and edited it. R.C.M. and T.C.S. directed and coordinated the project. This work was supported by NIH grants MH086403 (R.C.M., T.C.S.) and MH063394 (R.C.M.). A.J.M.M. was supported by a José Castillejo Postdoctoral Fellowship (I-D+i 2008-2011) from the Spanish Ministry of Education.

Accepted: November 30, 2012
Published: February 6, 2013

REFERENCES

Adesnik, H., Nicoll, R.A., and England, P.M. (2005). Photoinactivation of native AMPA receptors reveals their real-time trafficking. Neuron *48*, 977–985.

Ahmad, M., Polepalli, J.S., Goswami, D., Yang, X., Kaeser-Woo, Y.J., Südhof, T.C., and Malenka, R.C. (2012). Postsynaptic complexin controls AMPA receptor exocytosis during LTP. Neuron *73*, 260–267.

Blasi, J., Chapman, E.R., Link, E., Binz, T., Yamasaki, S., De Camilli, P., Südhof, T.C., Niemann, H., and Jahn, R. (1993). Botulinum neurotoxin A selectively cleaves the synaptic protein SNAP-25. Nature *365*, 160–163.

Bredt, D.S., and Nicoll, R.A. (2003). AMPA receptor trafficking at excitatory synapses. Neuron *40*, 361–379.

Clapp, W.C., Hamm, J.P., Kirk, I.J., and Teyler, T.J. (2012). Translating long-term potentiation from animals to humans: a novel method for noninvasive assessment of cortical plasticity. Biol. Psychiatry *71*, 496–502.

Collingridge, G.L., Isaac, J.T., and Wang, Y.T. (2004). Receptor trafficking and synaptic plasticity. Nat. Rev. Neurosci. *5*, 952–962.

Correia, S.S., Bassani, S., Brown, T.C., Lisé, M.F., Backos, D.S., El-Husseini, A., Passafaro, M., and Esteban, J.A. (2008). Motor protein-dependent transport of AMPA receptors into spines during long-term potentiation. Nat. Neurosci. *11*, 457–466.

Ehlers, M.D. (2012). Hijacking hebb: noninvasive methods to probe plasticity in psychiatric disease. Biol. Psychiatry *71*, 484–486.

Fasshauer, D., Antonin, W., Margittai, M., Pabst, S., and Jahn, R. (1999). Mixed and non-cognate SNARE complexes. Characterization of assembly and biophysical properties. J. Biol. Chem. *274*, 15440–15446.

Fernández-Chacón, R., Königstorfer, A., Gerber, S.H., García, J., Matos, M.F., Stevens, C.F., Brose, N., Rizo, J., Rosenmund, C., and Südhof, T.C. (2001). Synaptotagmin I functions as a calcium regulator of release probability. Nature *410*, 41–49.

Giraudo, C.G., Eng, W.S., Melia, T.J., and Rothman, J.E. (2006). A clamping mechanism involved in SNARE-dependent exocytosis. Science *313*, 676–680.

Gustafsson, M.G., Shao, L., Carlton, P.M., Wang, C.J., Golubovskaya, I.N., Cande, W.Z., Agard, D.A., and Sedat, J.W. (2008). Three-dimensional resolution doubling in wide-field fluorescence microscopy by structured illumination. Biophys. J. *94*, 4957–4970.

Hayashi, T., McMahon, H., Yamasaki, S., Binz, T., Hata, Y., Südhof, T.C., and Niemann, H. (1994). Synaptic vesicle membrane fusion complex: action of clostridial neurotoxins on assembly. EMBO J. *13*, 5051–5061.

Henley, J.M., Barker, E.A., and Glebov, O.O. (2011). Routes, destinations and delays: recent advances in AMPA receptor trafficking. Trends Neurosci. *34*, 258–268.

Holt, M., Varoqueaux, F., Wiederhold, K., Takamori, S., Urlaub, H., Fasshauer, D., and Jahn, R. (2006). Identification of SNAP-47, a novel Qbc-SNARE with ubiquitous expression. J. Biol. Chem. *281*, 17076–17083.

Huntwork, S., and Littleton, J.T. (2007). A complexin fusion clamp regulates spontaneous neurotransmitter release and synaptic growth. Nat. Neurosci. *10*, 1235–1237.

Jahn, R., and Scheller, R.H. (2006). SNAREs–engines for membrane fusion. Nat. Rev. Mol. Cell Biol. *9*, 631–643.

Jahn, R., Lang, T., and Südhof, T.C. (2003). Membrane fusion. Cell *112*, 519–533.

Kauer, J.A., and Malenka, R.C. (2007). Synaptic plasticity and addiction. Nat. Rev. Neurosci. *8*, 844–858.

Kennedy, M.J., and Ehlers, M.D. (2011). Mechanisms and function of dendritic exocytosis. Neuron *69*, 856–875.

Kennedy, M.J., Davison, I.G., Robinson, C.G., and Ehlers, M.D. (2010). Syntaxin-4 defines a domain for activity-dependent exocytosis in dendritic spines. Cell *141*, 524–535.

Khvotchev, M., Dulubova, I., Sun, J., Dai, H., Rizo, J., and Südhof, T.C. (2007). Dual modes of Munc18-1/SNARE interactions are coupled by functionally critical binding to syntaxin-1 N terminus. J. Neurosci. *27*, 12147–12155.

Kopec, C.D., Li, B., Wei, W., Boehm, J., and Malinow, R. (2006). Glutamate receptor exocytosis and spine enlargement during chemically induced long-term potentiation. J. Neurosci. *26*, 2000–2009.

Kopec, C.D., Real, E., Kessels, H.W., and Malinow, R. (2007). GluR1 links structural and functional plasticity at excitatory synapses. J. Neurosci. *27*, 13706–13718.

Lau, C.G., Takayasu, Y., Rodenas-Ruano, A., Paternain, A.V., Lerma, J., Bennett, M.V., and Zukin, R.S. (2010). SNAP-25 is a target of protein kinase

C phosphorylation critical to NMDA receptor trafficking. J. Neurosci. *30*, 242–254.

Lin, D.T., Makino, Y., Sharma, K., Hayashi, T., Neve, R., Takamiya, K., and Huganir, R.L. (2009). Regulation of AMPA receptor extrasynaptic insertion by 4.1N, phosphorylation and palmitoylation. Nat. Neurosci. *7*, 879–887.

Lledo, P.M., Zhang, X., Südhof, T.C., Malenka, R.C., and Nicoll, R.A. (1998). Postsynaptic membrane fusion and long-term potentiation. Science *279*, 399–403.

Lu, W., Man, H., Ju, W., Trimble, W.S., MacDonald, J.F., and Wang, Y.T. (2001). Activation of synaptic NMDA receptors induces membrane insertion of new AMPA receptors and LTP in cultured hippocampal neurons. Neuron *29*, 243–254.

Lu, J., Helton, T.D., Blanpied, T.A., Rácz, B., Newpher, T.M., Weinberg, R.J., and Ehlers, M.D. (2007). Postsynaptic positioning of endocytic zones and AMPA receptor cycling by physical coupling of dynamin-3 to Homer. Neuron *55*, 874–889.

Lüscher, C., Xia, H., Beattie, E.C., Carroll, R.C., von Zastrow, M., Malenka, R.C., and Nicoll, R.A. (1999). Role of AMPA receptor cycling in synaptic transmission and plasticity. Neuron *24*, 649–658.

Makino, H., and Malinow, R. (2009). AMPA receptor incorporation into synapses during LTP: the role of lateral movement and exocytosis. Neuron *64*, 381–390.

Malenka, R.C., and Bear, M.F. (2004). LTP and LTD: an embarrassment of riches. Neuron *44*, 5–21.

Malenka, R.C., and Nicoll, R.A. (1999). Long-term potentiation—a decade of progress? Science *285*, 1870–1874.

Malinow, R., and Malenka, R.C. (2002). AMPA receptor trafficking and synaptic plasticity. Annu. Rev. Neurosci. *25*, 103–126.

Maximov, A., Tang, J., Yang, X., Pang, Z.P., and Südhof, T.C. (2009). Complexin controls the force transfer from SNARE complexes to membranes in fusion. Science *323*, 516–521.

McMahon, H.T., Missler, M., Li, C., and Südhof, T.C. (1995). Complexins: cytosolic proteins that regulate SNAP receptor function. Cell *83*, 111–119.

Neves, G., Cooke, S.F., and Bliss, T.V. (2008). Synaptic plasticity, memory and the hippocampus: a neural network approach to causality. Nat. Rev. Neurosci. *9*, 65–75.

Newpher, T.M., and Ehlers, M.D. (2008). Glutamate receptor dynamics in dendritic microdomains. Neuron *58*, 472–497.

Opazo, P., and Choquet, D. (2011). A three-step model for the synaptic recruitment of AMPA receptors. Mol. Cell. Neurosci. *46*, 1–8.

Opazo, P., Labrecque, S., Tigaret, C.M., Frouin, A., Wiseman, P.W., De Koninck, P., and Choquet, D. (2010). CaMKII triggers the diffusional trapping of surface AMPARs through phosphorylation of stargazin. Neuron *67*, 239–252.

Pabst, S., Hazzard, J.W., Antonin, W., Südhof, T.C., Jahn, R., Rizo, J., and Fasshauer, D. (2000). Selective interaction of complexin with the neuronal SNARE complex. Determination of the binding regions. J. Biol. Chem. *275*, 19808–19818.

Pang, Z.P., Cao, P., Xu, W., and Südhof, T.C. (2010). Calmodulin controls synaptic strength via presynaptic activation of calmodulin kinase II. J. Neurosci. *30*, 4132–4142.

Park, M., Penick, E.C., Edwards, J.G., Kauer, J.A., and Ehlers, M.D. (2004). Recycling endosomes supply AMPA receptors for LTP. Science *305*, 1972–1975.

Passafaro, M., Piëch, V., and Sheng, M. (2001). Subunit-specific temporal and spatial patterns of AMPA receptor exocytosis in hippocampal neurons. Nat. Neurosci. *4*, 917–926.

Patterson, M.A., Szatmari, E.M., and Yasuda, R. (2010). AMPA receptors are exocytosed in stimulated spines and adjacent dendrites in a Ras-ERK-dependent manner during long-term potentiation. Proc. Natl. Acad. Sci. USA *107*, 15951–15956.

Petrini, E.M., Lu, J., Cognet, L., Lounis, B., Ehlers, M.D., and Choquet, D. (2009). Endocytic trafficking and recycling maintain a pool of mobile surface AMPA receptors required for synaptic potentiation. Neuron *63*, 92–105.

Puthenveedu, M.A., Lauffer, B., Temkin, P., Vistein, R., Carlton, P., Thorn, K., Taunton, J., Weiner, O.D., Parton, R.G., and von Zastrow, M. (2010). Sequence-dependent sorting of recycling proteins by actin-stabilized endosomal microdomains. Cell *143*, 761–773.

Reim, K., Mansour, M., Varoqueaux, F., McMahon, H.T., Südhof, T.C., Brose, N., and Rosenmund, C. (2001). Complexins regulate a late step in Ca^{2+}-dependent neurotransmitter release. Cell *104*, 71–81.

Rizo, J., and Rosenmund, C. (2008). Synaptic vesicle fusion. Nat. Struct. Mol. Biol. *15*, 665–674.

Schiavo, G., Benfenati, F., Poulain, B., Rossetto, O., Polverino de Laureto, P., DasGupta, B.R., and Montecucco, C. (1992). Tetanus and botulinum-B neurotoxins block neurotransmitter release by proteolytic cleavage of synaptobrevin. Nature *359*, 832–835.

Schlüter, O.M., Xu, W., and Malenka, R.C. (2006). Alternative N-terminal domains of PSD-95 and SAP97 govern activity-dependent regulation of synaptic AMPA receptor function. Neuron *51*, 99–111.

Schoch, S., Deák, F., Königstorfer, A., Mozhayeva, M., Sara, Y., Südhof, T.C., and Kavalali, E.T. (2001). SNARE function analyzed in synaptobrevin/VAMP knockout mice. Science *294*, 1117–1122.

Sharma, M., Burré, J., and Südhof, T.C. (2011). CSPα promotes SNARE-complex assembly by chaperoning SNAP-25 during synaptic activity. Nat. Cell Biol. *13*, 30–39.

Shen, J., Tareste, D.C., Paumet, F., Rothman, J.E., and Melia, T.J. (2007). Selective activation of cognate SNAREpins by Sec1/Munc18 proteins. Cell *128*, 183–195.

Shepherd, J.D., and Huganir, R.L. (2007). The cell biology of synaptic plasticity: AMPA receptor trafficking. Annu. Rev. Cell Dev. Biol. *23*, 613–643.

Soler-Llavina, G.J., Fuccillo, M.V., Ko, J., Südhof, T.C., and Malenka, R.C. (2011). The neurexin ligands, neuroligins and leucine-rich repeat transmembrane proteins, perform convergent and divergent synaptic functions in vivo. Proc. Natl. Acad. Sci. USA *108*, 16502–16509.

Südhof, T.C. (2004). The synaptic vesicle cycle. Annu. Rev. Neurosci. *27*, 509–547.

Südhof, T.C. (2012). The presynaptic active zone. Neuron *75*, 11–25.

Südhof, T.C., and Rothman, J.E. (2009). Membrane fusion: grappling with SNARE and SM proteins. Science *323*, 474–477.

Suh, Y.H., Terashima, A., Petralia, R.S., Wenthold, R.J., Isaac, J.T., Roche, K.W., and Roche, P.A. (2010). A neuronal role for SNAP-23 in postsynaptic glutamate receptor trafficking. Nat. Neurosci. *13*, 338–343.

Sutton, R.B., Fasshauer, D., Jahn, R., and Brunger, A.T. (1998). Crystal structure of a SNARE complex involved in synaptic exocytosis at 2.4 A resolution. Nature *395*, 347–353.

Tanaka, H., and Hirano, T. (2012). Visualization of subunit-specific delivery of glutamate receptors to postsynaptic membrane during hippocampal long-term Potentiation. Cell Rep. *1*, 291–298.

Tang, J., Maximov, A., Shin, O.H., Dai, H., Rizo, J., and Südhof, T.C. (2006). A complexin/synaptotagmin 1 switch controls fast synaptic vesicle exocytosis. Cell *126*, 1175–1187.

Temkin, P., Lauffer, B., Jäger, S., Cimermancic, P., Krogan, N.J., and von Zastrow, M. (2011). SNX27 mediates retromer tubule entry and endosome-to-plasma membrane trafficking of signalling receptors. Nat. Cell Biol. *13*, 715–721.

Verhage, M., Maia, A.S., Plomp, J.J., Brussaard, A.B., Heeroma, J.H., Vermeer, H., Toonen, R.F., Hammer, R.E., van den Berg, T.K., Missler, M., et al. (2000). Synaptic assembly of the brain in the absence of neurotransmitter secretion. Science *287*, 864–869.

Wang, Z., Edwards, J.G., Riley, N., Provance, D.W., Jr., Karcher, R., Li, X.D., Davison, I.G., Ikebe, M., Mercer, J.A., Kauer, J.A., and Ehlers, M.D. (2008).

Myosin Vb mobilizes recycling endosomes and AMPA receptors for postsynaptic plasticity. Cell *135*, 535–548.

Xu, W., Schlüter, O.M., Steiner, P., Czervionke, B.L., Sabatini, B., and Malenka, R.C. (2008). Molecular dissociation of the role of PSD-95 in regulating synaptic strength and LTD. Neuron *57*, 248–262.

Xue, M., Stradomska, A., Chen, H., Brose, N., Zhang, W., Rosenmund, C., and Reim, K. (2008). Complexins facilitate neurotransmitter release at excitatory and inhibitory synapses in mammalian central nervous system. Proc. Natl. Acad. Sci. USA *105*, 7875–7880.

Xue, M., Lin, Y.Q., Pan, H., Reim, K., Deng, H., Bellen, H.J., and Rosenmund, C. (2009). Tilting the balance between facilitatory and inhibitory functions of mammalian and Drosophila Complexins orchestrates synaptic vesicle exocytosis. Neuron *64*, 367–380.

Yang, B., Gonzalez, L., Jr., Prekeris, R., Steegmaier, M., Advani, R.J., and Scheller, R.H. (1999). SNARE interactions are not selective. Implications for membrane fusion specificity. J. Biol. Chem. *274*, 5649–5653.

Yang, Y., Wang, X.B., Frerking, M., and Zhou, Q. (2008). Delivery of AMPA receptors to perisynaptic sites precedes the full expression of long-term potentiation. Proc. Natl. Acad. Sci. USA *105*, 11388–11393.

Yang, X., Kaeser-Woo, Y.J., Pang, Z.P., Xu, W., and Südhof, T.C. (2010). Complexin clamps asynchronous release by blocking a secondary Ca^{2+} sensor via its accessory α helix. Neuron *68*, 907–920.

Yudowski, G.A., Puthenveedu, M.A., Leonoudakis, D., Panicker, S., Thorn, K.S., Beattie, E.C., and von Zastrow, M. (2007). Real-time imaging of discrete exocytic events mediating surface delivery of AMPA receptors. J. Neurosci. *27*, 11112–11121.